ISSN: 0067-2904

New Analytical and Numerical Solutions for Squeezing Flow between Parallel Plates under Slip

Hassan Raheem Shool[1*], Ahmed K. Al-Jaberi[1] and Abeer Majeed Jasim[2]
[1]Department of Mathematics, College of Education for pure Science, University of Basra, Basra, Iraq.
[2]Department of Mathematics, College of Science, University of Basra. Basra, Iraq.

Received: 7/2/2023 Accepted: 2/4/2023 Published: 30/3/2024

Abstract

In this article, the effects of physical flow parameters on squeezed fluid between parallel plates are explored through the Darcy porous channel when fluid is moving as a result of the upper plate being squeezed towards the stretchable lower plate, such as velocity slip, thermal slip, solutal slip, thermal stratification parameter, solutal stratification parameter, squeezing number, Darcy number, Prandtl number, and Schmidt number. The governing equations are transformed into a nonlinear ordinary differential equation using the appropriate similarity transformations. The resulting equations are solved by using the perturbation iteration method (PIT) to produce a convergent analytical solution with high accuracy. The phenomena of the squeezing fluid as the plates are moving apart and when they are coming together are illustrated using the resulting analytical solutions. Plots are used to discuss the significant effects of physical parameters on velocity, temperature, and fluid concentration profiles. The skin friction coefficient and Nusselt Sherwood values have graphical interpretations that are listed. For strong velocity slip parameters, the results demonstrate the existence of a minimum velocity profile close to the plate and a growing velocity profile distant from the plate. Additionally, as the slip effects rise, the fluid temperature and concentration both considerably drop. The results of the fourth-order Runge-Kutta method ($RK4^M$) and the presented analytical solutions provided are in excellent agreement.

Keywords: Squeezing flow, Slips conditions, Ordinary differential equation, Perturbation iteration algorithm.

حلول تحليلية وعددية جديدة لضغط التدفق بين صفائح متوازية تحت الانزلاق

حسن رحيم شول[1*] ، احمد كاظم الجابري[2] ، عبير مجيد جاسم[3]
[1]قسم الرياضيات، كلية التربية للعلوم الصرفة، جامعة البصرة، البصرة، العراق،
[2] قسم الرياضيات، كلية العلوم، جامعة البصرة، البصرة، العراق،

الخلاصة

في هذا المقال استكشاف لتاثيرات معاملات التدفق الفيزيائي على السوائل المضغوطة بين الصفائح المتوازية من خلال قناة دارسي المسامية عندما يتحرك السائل نتيجة الضغط على الصفيحة العلوية نحو الصفيحة السفلية القابلة للمط، مثل انزلاق السرعة، الانزلاق الحراري، الانزلاق المذاب، معامل التقسيم الحراري، معامل التقسيم الطبقي، الضغط، رقم دارسي، رقم براندل ورقم شميدت، تم تحويل المعادلات الحاكمة الى

Email: ahmed.shanan@uobasrah.edu.iq

معدلة تفاضلية اعتيادية غير خطية باستخدام تحويلات تشابه مناسبة و حل المعادلة الناتجة باستخدام طريقة تكرار الاضطراب (PIT) للحصول
على حل تحليلي متقارب بدقة متزايدة. يتم توضيح ظاهرة سائل الضغط اثناء تحرك الصفائح حين تتباعد وتلتقي معا باستخدام الحلول التحليلية المكتسبة. استخدمت الاشكال البيانية لمناقشة التاثيرات الهامة للمعلمات الفيزيائية على السرعة، درجة الحرارة، تركيز السوائل، معامل احتكاك الجلد وقيم نسلت شيرود حيث يكون لها تفسيرات بيانية تم توضيحها. النتائج تبين وجود مجال سرعة متدني قريب من اللوحة ومجال سرعة متنامي بعيد عن اللوحة. بالاضافة الى ذلك عند ارتفاع تاثيرات الانزلاق تنخفض درجة حرارة السائل والتركيز بشكل كبير. كانت استنتاجات نتائج الحلول التحليلية متفقة مع نتائج تم الحصول عليها باستخدام طرق رانج كوتا من الرتبة الرابعة ($RK4^M$).

1. Introduction

The significance of slip effects among parallel plates in several fluid dynamic systems has attracted the attention of numerous researchers. In the literature, it was noticed that the majority of analyses were conducted assuming no slip circumstances existed on the surfaces. It is important to swap out the non-slip conditions with slip conditions in various physical situations where these conditions are no longer appropriate. Chemically treated or lubricated hydrophobic surfaces, shear skin, wire nettings, perforated plates, porous or rough surfaces, hysteresis and spurts effects, and the super-hydrophobic nano-surfaces have all demonstrated the importance of slip conditions. The fluid flow on many interfaces, polishing of mechanical heart valves, and issues with rarefied fluid are some other instances of industrial thermal issues that arise when slip occurs. Navier [1] and Maxwell [2] carried out earlier research on linear slip flow. The fluid flow under the influence of slip was presented by Rao and Rajagopal [3]. The impact of slip circumstances on the flow of the Casson fluid through a thermally stratified channel was covered by Hayat et al. [4]. Jasim [5] studied the exploration of no-slip and slip of unsteady squeezing flow fluid through a derivatives series algorithm. With slip circumstances and varying magnetic fields, Rana et al [6] illustrated nanofluid flow and heat transfer over a non-linear permeable sheet. Ullah and Zaman [7] talked about the Lie group analysis of tangent hyperbolic fluid flow in a stretching sheet under slip conditions. An unsteady squeezing flow of the Casson fluid having magnetohydrodynamic effect and passing through a porous medium channel with slip at the boundaries was modeled and analyzed by Mubashir et al. in [8]. Jasim [9] studied the effect of magnetohydrodynamics on squeezing flow in a porous medium of the Casson nanofluid between parallel plates using a new scheme technique. The effects of slip on fluid flow in porous media were presented by Moghaddam and Jamiolahmady [10]. Through temperature differences in the concentration of fluids with different densities, the phenomenon of double stratification is accomplished in many industrial and natural processes. The double-strategy method has Numerous scientific applications that may be made, as seen in Figure.1.

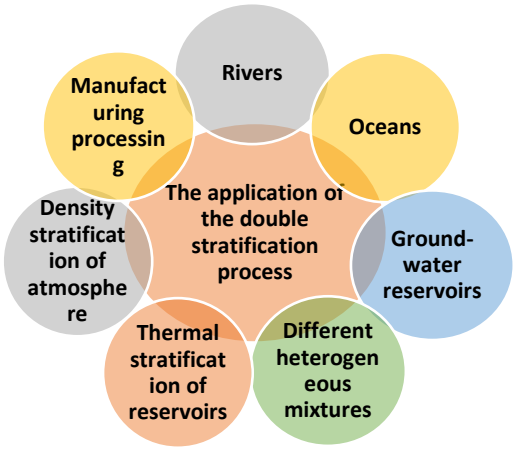

Fiqure.1: The application of the double stratification process.

The stratification procedure could be applied to energy storage and solar engineering. Additionally, the biological activities that occur in reservoirs result in anoxic bottom water. The existence of thermal radiation with copper-water nanofluid and the effect of heat transfer in unsteady magnetohydrodynamics squeezing and suction injection on the flow between parallel plates in a porous medium was discussed by Jasim [11]. The dual stratified UCM flow across a melting surface in the presence of double stratification and cross-diffusion effects was presented by Babu and Sandeep [12]. The mixed convection effects on double stratification over a vertical sheet inserted in a non-darcy Porous Media were presented by Srinivasachary and Surender [13]. According to the aforementioned publications, no attempt was made to exploit double stratification and the compound effects of slip (velocity, temperature, and solutal conditions) in squeezing flow analysis. In [14], the first attempt was made in 2018 to investigate the mass, heat, and Newtonian fluid of fluid flow through a porous medium with double stratification and slip conditions. The homotopy analysis method was used to discuss the slip analysis of squeezing flow using doubly stratified fluid. Also, Al-Khafajy and Al-Delfi [15] investigated the impact of an elastic wall on the peristaltic flow of fluid between two concentric cylinders with various parameters such as Reynolds number. We aim to use the perturbation iteration method and provide new initial conditions to extract a new approximate analytical solution through a porous medium with double stratification and slip conditions for the Newtonian fluid flow, continuity, momentum, and energy conservations. It is clear that from this work, the perturbation iteration technique is used for both the slip analysis of the squeezed flow between parallel plates as well as to find an analytical-approximate solution. Additionally, the effects of flow factors including the Eckert number, Schmidt number, solutal stratification parameter, thermal stratification parameter, and squeezing number are examined. The fourth-order Runge-Kutta method is used to compare the outcomes of the analytical solutions and the numerical method. The structure of this paper is as follows: In Section 2, the governing equations are derived. Section 3 of the paper describes how PIT applies incompressible and viscous fluid inside infinite parallel disks. Sections 4, 5, 6, and 7 provide discussions and findings. Section 8 contains the convergence analysis. Finally, section 9 provides the conclusions.

2- Mathematical formulation

Considering the incompressible and viscous fluid inside the infinite parallel disks, the two plates are separated by the distance $y = f(t) = \sqrt{\frac{\nu(1-\delta t)}{a}}$ apart, for $\delta > 0$, the two plates are

squeezed until they touch at $t = \frac{1}{\delta}$ and for $\delta < 0$, the two plates are separated. The motion of the fluid is assumed as unsteady and laminar subjected to a Darcy porous medium. It is assumed that the fluid's motion is laminar, unstable, and susceptible to a Darcy porous media. The flow is analyzed using the coordinate system (x, y), where the $\boldsymbol{x}$-axis is considered to run along the axis of the bottom plate and the $\boldsymbol{y}$-axis is directed ordinarily in its direction. As shown in Figure 2, it is assumed that the top fixed disk is being squeezed vertically with velocity $\ddot{v}_f$,while the bottom fixed disk is being stretched in a direction with velocity $\ddot{U}(x)$.

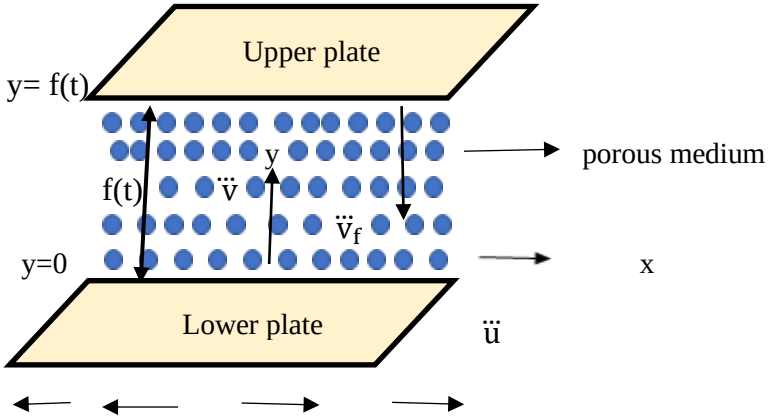

Figure 2: The geometry of the problem.

The governing equations of the unsteady two-dimensional flow of incompressible viscous fluid can be introduced as follows [16].

$$\frac{\partial \ddot{u}}{\partial \ddot{x}} + \frac{\partial \ddot{v}}{\partial \ddot{y}} = 0 \tag{1}$$

$$\frac{\partial \ddot{u}}{\partial \ddot{t}} + \ddot{u}\frac{\partial \ddot{u}}{\partial \ddot{x}} + \ddot{v}\frac{\partial \ddot{u}}{\partial \ddot{y}} = -\frac{1}{\tilde{\rho}}\frac{\partial \ddot{p}}{\partial \ddot{x}} + \nu\left(\frac{\partial^2 \ddot{u}}{\partial \ddot{x}^2} + \frac{\partial^2 \ddot{u}}{\partial \ddot{y}^2}\right) - \frac{\nu \phi^*}{k^*}\ddot{u} \tag{2}$$

$$\frac{\partial \ddot{v}}{\partial \ddot{t}} + \ddot{u}\frac{\partial \ddot{v}}{\partial \ddot{x}} + \ddot{v}\frac{\partial \ddot{v}}{\partial \ddot{y}} = -\frac{1}{\tilde{\rho}}\frac{\partial \ddot{p}}{\partial \ddot{y}} + \nu\left(\frac{\partial^2 \ddot{v}}{\partial \ddot{x}^2} + \frac{\partial^2 \ddot{v}}{\partial \ddot{y}^2}\right) - \frac{\nu \phi^*}{k^*}\ddot{v} \tag{3}$$

$$\frac{\partial \ddot{T}}{\partial \ddot{t}} + \ddot{u}\frac{\partial \ddot{T}}{\partial \ddot{x}} + \ddot{v}\frac{\partial \ddot{T}}{\partial \ddot{y}} = \alpha\left(\frac{\partial^2 \ddot{T}}{\partial \ddot{x}^2} + \frac{\partial^2 \ddot{T}}{\partial \ddot{y}^2}\right) \tag{4}$$

$$\frac{\partial \ddot{C}}{\partial \ddot{t}} + \ddot{u}\frac{\partial \ddot{C}}{\partial \ddot{x}} + \ddot{v}\frac{\partial \ddot{C}}{\partial \ddot{y}} = \ddot{D}\left(\frac{\partial^2 \ddot{C}}{\partial \ddot{x}^2} + \frac{\partial^2 \ddot{C}}{\partial \ddot{y}^2}\right) \tag{5}$$

Here, $\ddot{u}$ and $\ddot{v}$ are the velocity components in x and y direction, respectively. $\tilde{\rho}$ is the density, $\ddot{p}$ is the pressure, ν is the kinematics viscosity, ϕ^* is the porosity of porous medium, $k^*$is the permeability of the porous medium, $\ddot{T}$ is the temperature, $\alpha = \frac{K_0}{\tilde{\rho} C_p}$ is thermal diffusivity, K_0 is thermal conductivity, $C_p$is the specific heat, $\ddot{C}$ is the fluid concentration and $\ddot{D}$ is the diffusion coefficient. Appropriate boundary conditions are described as follows [9]:

$$\ddot{u} = \ddot{U}_w(x) + L\frac{\partial \ddot{u}}{\partial \ddot{y}}, \ddot{v} = 0, \ddot{T} = \ddot{T}_w(x) + K1\frac{\partial \ddot{T}}{\partial \ddot{y}}, \ddot{C} = \ddot{C}_w(x) + K2\frac{\partial \ddot{C}}{\partial \ddot{y}} \quad \text{at } y = 0,$$

$$\ddot{u} = 0, \ddot{v} = \ddot{v}_f = \frac{df}{dt} = -\frac{\delta}{2}\sqrt{\frac{\nu}{a(1-\delta t)}}, \ddot{T} = \ddot{T}_f(\ddot{x}), \ddot{C} = \ddot{C}_f(x) \quad \text{at } \ddot{y} = f(t),$$

$$\ddot{U}_w(\ddot{x}) = \frac{ax}{(1-\delta t)}, \ddot{T}_w(x) = \ddot{T}_0 + \frac{d\,x}{(1-\delta t)}, \ddot{C}_w(x) = \ddot{C}_0 + \frac{e\,x}{(1-\delta t)},$$

$$\ddot{T}_f(x) = \ddot{T}_0 + \frac{d_1\,x}{(1-\delta t)}, \ddot{C}_f(x) = \ddot{C}_0 + \frac{e_1\,x}{(1-\delta t)}, \tag{6}$$

$\ddot{U}_w(x)$ is the stretching velocity, L is the velocity slip factor, $\ddot{T}_w(x)$ is the variable surface temperature, $K1, \text{and } K2$ are the temperature slip factor and solutal slip factor, respectively.

$\ddot{C}_w(x)$ is the variable surface concentration, $\ddot{T}_f(x)$ is the variable upper plate e temperature, $\ddot{C}_f(x)$ is the variable upper plate concentration, $\ddot{T}_0$ is the reference temperature, $\ddot{C}_0$ is the reference concentration and $d, d_1, e, e_1, a, \delta$ are dimensional constants. By using the similarity transformations [17]

$$\varepsilon = \frac{y}{\sqrt{\frac{\nu(1-\delta\, t)}{a}}},\quad \Psi = \sqrt{\frac{a\nu}{(1-\delta t)}}\, x\, h(\varepsilon),\quad \chi(\varepsilon) = \frac{(\ddot{T}-\ddot{T}_f)}{\ddot{T}_w-\ddot{T}_0},\quad \kappa(\varepsilon) = \frac{(\ddot{C}-\ddot{C}_f)}{\ddot{C}_w-\ddot{C}_0}, \tag{7}$$

where ε is the similarity variable, Ψ is the stream function defined as, $\ddot{u} = \frac{\partial \Psi}{\partial \ddot{y}}$, $\ddot{v} = -\frac{\partial \Psi}{\partial \ddot{x}}$ which identically satisfies Equation (1). The functions $h(\varepsilon), \chi(\varepsilon)$ and $\kappa(\varepsilon)$ are dimensionless stream function, temperature function, and concentration function, respectively. Using Equation (7), we obtain

$$\ddot{u} = \ddot{U}_w(x)\frac{dh(\varepsilon)}{d\varepsilon}, \ddot{v} = -\sqrt{\frac{av}{(1-\delta\, t)}}\, h(\varepsilon)\,. \tag{8}$$

To eliminate pressure terms from the resulting equations, we differentiate Equation (2) for $\ddot{y}$ and Equation (3) for $\ddot{x}$,then we get:

$$\frac{\partial^2 \ddot{u}}{\partial \ddot{t}\,\partial \ddot{y}} + \ddot{u}\frac{\partial^2 \ddot{u}}{\partial \ddot{x}\,\partial \ddot{y}} + \frac{\partial \ddot{u}}{\partial \ddot{y}}\frac{\partial \ddot{u}}{\partial \ddot{x}} + \ddot{v}\frac{\partial^2 \ddot{u}}{\partial \ddot{y}^2} + \frac{\partial \ddot{v}}{\partial \ddot{y}}\frac{\partial \ddot{u}}{\partial \ddot{y}} = -\frac{1}{\tilde{\rho}}\frac{\partial^2 \ddot{p}}{\partial \ddot{x}\,\partial \ddot{y}} + \nu\left[\frac{\partial^3 \ddot{u}}{\partial \ddot{x}^2\,\partial \ddot{y}} + \frac{\partial^3 \ddot{u}}{\partial \ddot{y}^3}\right] - \frac{\nu\phi^*}{k^*}\frac{\partial \ddot{u}}{\partial \ddot{y}} \tag{9}$$

$$\frac{\partial^2 \ddot{v}}{\partial \ddot{t}\,\partial \ddot{x}} + \ddot{u}\frac{\partial^2 \ddot{v}}{\partial \ddot{x}^2} + \frac{\partial \ddot{u}}{\partial \ddot{x}}\frac{\partial \ddot{v}}{\partial \ddot{x}} + \ddot{v}\frac{\partial^2 \ddot{v}}{\partial \ddot{y}\,\partial \ddot{x}} + \frac{\partial \ddot{v}}{\partial \ddot{x}}\frac{\partial \ddot{v}}{\partial \ddot{y}} = -\frac{1}{\tilde{\rho}}\frac{\partial^2 \ddot{p}}{\partial \ddot{x}\,\partial \ddot{y}} + \nu\left[\frac{\partial^3 \ddot{v}}{\partial \ddot{x}^3} + \frac{\partial^3 \ddot{v}}{\partial \ddot{y}^2\,\partial \ddot{x}}\right] - \frac{\nu\phi^*}{k^*}\frac{\partial \ddot{v}}{\partial \ddot{y}} \tag{10}$$

(9-10) gives

$$\left(\frac{\partial^2 \ddot{u}}{\partial \ddot{t}\,\partial \ddot{y}} - \frac{\partial^2 \ddot{v}}{\partial \ddot{t}\,\partial \ddot{x}}\right) + \left(\ddot{u}\frac{\partial^2 \ddot{u}}{\partial \ddot{x}\,\partial \ddot{y}} - \ddot{u}\frac{\partial^2 \ddot{v}}{\partial \ddot{x}^2}\right) + \left(\frac{\partial \ddot{u}}{\partial \ddot{y}}\frac{\partial \ddot{u}}{\partial \ddot{x}} - \frac{\partial \ddot{u}}{\partial \ddot{x}}\frac{\partial \ddot{v}}{\partial \ddot{x}}\right) + \left(\ddot{v}\frac{\partial^2 \ddot{u}}{\partial \ddot{y}^2} - \ddot{v}\frac{\partial^2 \ddot{v}}{\partial \ddot{y}\,\partial \ddot{x}}\right) + \left(\frac{\partial \ddot{v}}{\partial \ddot{y}}\frac{\partial \ddot{u}}{\partial \ddot{y}} - \frac{\partial \ddot{v}}{\partial \ddot{x}}\frac{\partial \ddot{v}}{\partial \ddot{y}}\right) =$$
$$\nu\left[\left(\frac{\partial^3 \ddot{u}}{\partial \ddot{x}^2\,\partial \ddot{y}} - \frac{\partial^3 \ddot{v}}{\partial \ddot{x}^3}\right) + \left(\frac{\partial^3 \ddot{u}}{\partial \ddot{y}^3} - \frac{\partial^3 \ddot{v}}{\partial \ddot{y}^2\,\partial \ddot{x}}\right)\right] - \frac{\nu\phi^*}{k^*}\left(\frac{\partial \ddot{u}}{\partial \ddot{y}} - \frac{\partial \ddot{v}}{\partial \ddot{y}}\right). \tag{11}$$

By using the similarity transformations Equation (7) and Equation (8), then finding the derivatives to them in Eq. (11), Eq. (4), and Eq. (5) , we get

$$\frac{d^4 h(\varepsilon)}{d\varepsilon^4} + h(\varepsilon)\frac{d^3 h(\varepsilon)}{d\varepsilon^3} - \frac{dh(\varepsilon)}{d\varepsilon}\frac{d^2 h(\varepsilon)}{d\varepsilon^2} - \frac{1}{2}Sq\left(3\frac{d^2 h(\varepsilon)}{d\varepsilon^2} - \varepsilon\frac{d^3 h(\varepsilon)}{d\varepsilon^3}\right) - \frac{1}{Da}\frac{d^2 h(\varepsilon)}{d\varepsilon^2} = 0, \tag{12}$$

$$\frac{d^2 \chi(\varepsilon)}{d\varepsilon^2} + \Pr\left(h(\varepsilon)\frac{d\chi(\varepsilon)}{d\varepsilon} - \chi(\varepsilon)\frac{dh(\varepsilon)}{d\varepsilon}\right) - \Pr Sq\left(K1 + \chi(\varepsilon)\right) - \Pr\left(\frac{1}{2}Sq\,\varepsilon\frac{d\chi(\varepsilon)}{d\varepsilon} + K1\frac{dh(\varepsilon)}{d\varepsilon}\right) = 0, \tag{13}$$

$$\frac{d^2 \kappa(\varepsilon)}{d\varepsilon^2} + Sc\left(h(\varepsilon)\frac{d\kappa(\varepsilon)}{d\varepsilon} - \kappa(\varepsilon)\frac{dh(\varepsilon)}{d\varepsilon}\right) - Sc\, Sq\left(K2 + \kappa(\varepsilon)\right) - Sc\left(\frac{1}{2}Sq\,\varepsilon\frac{d\kappa(\varepsilon)}{d\varepsilon} + K2\frac{dh(\varepsilon)}{d\varepsilon}\right) = 0, \tag{14}$$

Sq is the squeezing parameter, Da is a Darcy number, Pr is the Prandtl number, K1 is the thermal stratification parameter, Sc is the Schmidt number, and K2 is the solutal stratification parameter. The group of boundary conditions:

$$h(0) = 0,\ \frac{dh(0)}{d\varepsilon} = 1 + S_1\frac{d^2 h(0)}{d\varepsilon^2},\quad h(1) = \frac{1}{2}Sq,\quad \frac{dh(1)}{d\varepsilon} = 0, \tag{a15}$$

$$\chi(0) = 1 - K1 + S_2\frac{d\chi(0)}{d\varepsilon},\ \chi(1) = 0,\ \kappa(0) = 1 - K2 + S_3\frac{d\kappa(0)}{d\varepsilon},\ \kappa(1) = 0. \tag{b15}$$

Here, S_1, S_2 and S_3 are velocity slip, thermal slip, and solutal slip parameters, respectively.

$$Sq = \frac{\delta}{a},\ Da = \frac{k^* a}{\nu(1-\delta t)\varphi(\varepsilon)},\ \Pr = \frac{\nu}{\alpha},\ K1 = \frac{d_1}{d},\ K2 = \frac{e_1}{e},\ Sc = \frac{\nu}{d},$$
$$S_1 = L\sqrt{\frac{a}{\nu(1-\delta t)}}\,,\ S_2 = K1\sqrt{\frac{a}{\nu(1-\delta t)}}\,,\ S_3 = K2\sqrt{\frac{a}{\nu(1-\delta t)}}\,, \tag{16}$$

The plates are moving apart for $Sq > 0$ and toward one another for $Sq < 0$. When $K1 = K2 = 0$, stratification effects disappeared. As a result, the flow issue under consideration becomes a wall temperature issue. Additionally, the no-slip conditions for $S_1 = S_2 = S_3 = 0$

are recovered. The following information is provided for the skin friction coefficient, Nusselt number, and Sherwood number [12].

$\mathrm{Cf} = \frac{\tilde{\mu}\tau_{xy}|_{\mathrm{y=f(t)}}}{\tilde{\rho}(\ddot{U}_w(\ddot{x}))^2}$, $\mathrm{Nu} = \frac{-x\,\mathrm{K_0}\left(\frac{\partial \ddot{T}}{\partial \ddot{y}}\right)|_{\mathrm{y=f(t)}}}{\mathrm{K_0}(\ddot{T}_w - \ddot{T}_f)}$, $\mathrm{Sh} = \frac{-\ddot{x}\,\mathrm{D}\left(\frac{\partial \ddot{C}}{\partial \ddot{y}}\right)|_{\mathrm{y=f(t)}}}{\mathrm{D}\,(\ddot{C}_w - \ddot{C}_f)}$, $\mathrm{R}=\frac{\mathrm{x}\,\ddot{U}_w(x)}{v}$.

R is Reynolds number and from the above equations, yield

$\sqrt{Re}\,\mathrm{Cf} = \frac{\mathrm{d}^2\mathrm{h}(1)}{\mathrm{d}\varepsilon^2}$, $\frac{\mathrm{Nu}}{\sqrt{\mathrm{Re}}} = -(\frac{1}{1-\mathrm{K1}})\frac{\mathrm{d}\chi(1)}{\mathrm{d}\varepsilon}$, $\frac{\mathrm{Sh}}{\sqrt{\mathrm{Re}}} = -(\frac{1}{1-\mathrm{K2}})\frac{\mathrm{d}\kappa(1)}{\mathrm{d}\varepsilon}$,

3. The Application of squeezing flow between parallel disks by using PIT.

The PIT (1,1) is implemented to the nonlinear ordinary differential equations (12)-(14) using the foundations of its method to approximate slip analysis for two dimensional in the unsteady incompressible viscous fluid between parallel plates. The following is an illustration of the auxiliary perturbation parameter that can be displayed:

$\mathrm{G_1}\left(\mathrm{h}, \frac{\mathrm{d}^2\mathrm{h}}{\mathrm{d}\varepsilon^2}, \frac{\mathrm{d}^3\mathrm{h}}{\mathrm{d}\varepsilon^3}, \frac{\mathrm{d}^4\mathrm{h}}{\mathrm{d}\varepsilon^4}, \gamma\right) = \frac{\mathrm{d}^4\mathrm{h}}{\mathrm{d}\varepsilon^4} + \gamma\left(\mathrm{h}\frac{\mathrm{d}^3\mathrm{h}}{\mathrm{d}\varepsilon^3} - \frac{\mathrm{dh}}{\mathrm{d}\mathcal{E}}\frac{\mathrm{d}^2\mathrm{h}}{\mathrm{d}\varepsilon^2}\right) - \frac{1}{2}\gamma\,\mathrm{Sq}\left(3\frac{\mathrm{d}^2\mathrm{h}}{\mathrm{d}\varepsilon^2} - \varepsilon\frac{\mathrm{d}^3\mathrm{h}}{\mathrm{d}\varepsilon^3}\right) - \frac{\gamma}{\mathrm{D}_a}\frac{\mathrm{d}^2\mathrm{h}}{\mathrm{d}\varepsilon^2}$, (17)

$\mathrm{G_2}\left(\mathrm{h}, \frac{\mathrm{dh}}{\mathrm{d}\varepsilon}, \chi, \frac{\mathrm{d}\chi}{\mathrm{d}\varepsilon}, \frac{\mathrm{d}^2\chi}{\mathrm{d}\varepsilon^2}, \gamma\right) = \frac{\mathrm{d}^2\chi}{\mathrm{d}\varepsilon^2} + \gamma\,\mathrm{Pr}\left(\mathrm{h}\frac{\mathrm{d}\chi}{\mathrm{d}\mathcal{E}} - \mathrm{g}\frac{\mathrm{dh}}{\mathrm{d}\varepsilon}\right) - \gamma\mathrm{Pr}Sq(\mathrm{K1}+\chi) - \gamma\mathrm{Pr}\left(\frac{1}{2}\mathrm{Sq}\varepsilon\frac{\mathrm{d}\chi}{\mathrm{d}\mathcal{E}} + \mathrm{K1}\frac{\mathrm{dh}}{\mathrm{d}\mathcal{E}}\right)$, (18)

$\mathrm{G_3}\left(\mathrm{h}, \frac{\mathrm{dh}}{\mathrm{d}\varepsilon}, \kappa, \frac{\mathrm{d}\kappa}{\mathrm{d}\varepsilon}, \frac{\mathrm{d}^2\kappa}{\mathrm{d}\varepsilon^2}, \gamma\right) = \frac{\mathrm{d}^2\kappa}{\mathrm{d}\varepsilon^2} + \gamma\,\mathrm{Sc}\left(\mathrm{h}\frac{\mathrm{d}\kappa}{\mathrm{d}\mathcal{E}} - \kappa\frac{\mathrm{dh}}{\mathrm{d}\varepsilon}\right) - \gamma\,\mathrm{Sc}\,Sq(\mathrm{K2}+\kappa) - \gamma\,\mathrm{Sc}\left(\frac{1}{2}\mathrm{Sq}\,\varepsilon\frac{\mathrm{d}\kappa}{\mathrm{d}\mathcal{E}} + \mathrm{K2}\frac{\mathrm{dh}}{\mathrm{d}\mathcal{E}}\right)$ (19)

The definition of the perturbation expansions with only one correction term becomes

$$\mathrm{h_{n+1}} = \mathrm{h_n} + \gamma(\mathrm{h_c})_\mathrm{n}, \quad (20)$$

$$\chi_{\mathrm{n+1}} = \chi_\mathrm{n} + \gamma(\chi_\mathrm{c})_\mathrm{n}, \quad (21)$$

$$\kappa_{\mathrm{n+1}} = \kappa_\mathrm{n} + \gamma(\kappa_\mathrm{c})_\mathrm{n}, \quad (22)$$

Where n is the nth iteration, $\mathrm{h_c}$, χ_c and κ_c are correction terms in perturbation expansions. Substituting Equations (20)-(22) into Equations (17)-(19) respectively. Then expanding the resulting equations in a Taylor series with first-order derivative terms about $\gamma = 0$.

$\mathrm{G_1}(\mathrm{h_n}, \mathrm{h'_n}, \mathrm{h''_n}, \mathrm{h'''_n}, \mathrm{h''''_n}, 0) + \gamma\left[\mathrm{G_{1_{h_n}}}(\mathrm{h_c})_\mathrm{n} + \mathrm{G_{1_{h'_n}}}(\mathrm{h'_c})_\mathrm{n} + \mathrm{G_{1_{h''_n}}}(\mathrm{h''_c})_\mathrm{n} + \mathrm{G_{1_{h'''_n}}}(\mathrm{h'''_c})_\mathrm{n} + \mathrm{G_{1_{h''''_n}}}(\mathrm{h''''_c})_\mathrm{n} + \mathrm{G_{1_\gamma}}\right] = 0$ (23)

$\mathrm{G_2}(\mathrm{h_n}, \mathrm{h'_n}, \chi_\mathrm{n}, \chi'_\mathrm{n}, \chi''_\mathrm{n}, 0) + \gamma\left[\mathrm{G_{2_{h_n}}}(\mathrm{h_c})_\mathrm{n} + \mathrm{G_{2_{h'_n}}}(\mathrm{h'_c})_\mathrm{n} + \mathrm{G_{2_{\chi_n}}}(\chi_\mathrm{c})_\mathrm{n} + \mathrm{G_{2_{\chi'_n}}}(\chi'_\mathrm{c})_\mathrm{n} + \mathrm{G_{2_{\chi''_n}}}(\chi''_\mathrm{c})_\mathrm{n} + \mathrm{G_{2_\gamma}}\right] = 0,$ (24)

$\mathrm{G_3}(\mathrm{h_n}, \mathrm{h'_n}, \kappa_\mathrm{n}, \kappa'_\mathrm{n}, \kappa''_\mathrm{n}, 0) + \gamma\left[\mathrm{G_{3_{h_n}}}(\mathrm{h_c})_\mathrm{n} + \mathrm{G_{3_{h'_n}}}(\mathrm{h'_c})_\mathrm{n} + \mathrm{G_{3_{\kappa_n}}}(\kappa_\mathrm{c})_\mathrm{n} + \mathrm{G_{3_{\kappa'_n}}}(\kappa'_\mathrm{c})_\mathrm{n} + \mathrm{G_{3_{\kappa''_n}}}(\kappa''_\mathrm{c})_\mathrm{n} + \mathrm{G_{3_\gamma}}\right] = 0,$ (25)

The calculation of all derivatives is as follows:

$\mathrm{G_1}(\mathrm{h_n}, \mathrm{h'_n}, \mathrm{h''_n}, \mathrm{h'''_n}, \mathrm{h''''_n}, 0) = \mathrm{h''''_n}$, $\mathrm{G_{1_{h_n}}} = \gamma\,\mathrm{h'''_n}, \mathrm{G_{1_{h'_n}}} = -\gamma\mathrm{h''_n}$, $\mathrm{G_{1_{h''_n}}} = -\gamma\mathrm{h'_n} - \frac{3}{2}\gamma\mathrm{Sq} - \frac{\gamma}{\mathrm{D}_a}$,

$\mathrm{G_{1_{h'''_n}}} = \gamma\mathrm{h_n} + \frac{1}{2}Sq\varepsilon$, $\mathrm{G_{1_{h''''_n}}} = 1$, $\mathrm{G_{1_\gamma}} = (\mathrm{h\,h'''_n} - \mathrm{h'_n h''_n}) - \frac{1}{2}\mathrm{S_q}(3\mathrm{h''_n} - \varepsilon\mathrm{h'''_n}) - \frac{1}{\mathrm{D}_a}\mathrm{h''_n}$,

$\mathrm{G_2}(\mathrm{h_n}, \mathrm{h'_n}, \chi_\mathrm{n}, \chi'_\mathrm{n}, \chi''_\mathrm{n}, 0) = \chi''_\mathrm{n}$, $\mathrm{G_{2_{h_n}}} = \gamma\mathrm{Pr}\chi'_\mathrm{n}$, $\mathrm{G_{2_{h'_n}}} = -\gamma\,\mathrm{Pr}\,\chi_\mathrm{n} - \gamma\mathrm{PrK1}$, $\mathrm{G_{2_{\chi_n}}} = -\gamma\mathrm{Prh'_n} - \gamma\,\mathrm{Pr}\,\mathrm{Sq})$

$G_{2_{\chi_n'}} = \gamma Pr\, h_n - \frac{1}{2}\gamma PrSq\varepsilon,\ G_{2_{\chi_n''}} = 1,\ G_{2_\gamma} = Pr(h_n\chi_n' - \chi_n h_n') - PrSq(K1 + \chi_n) - Pr\left(\frac{1}{2}Sq\varepsilon\chi_n' + K1h_n'\right)$, $G_3(h_n, h_n', \kappa_n, \kappa_n', \kappa_n'', 0) = \kappa_n'',\quad G_{3_{h_n}} = \gamma Sc\, g_n',\ G_{3_{h_n'}} = -\gamma\, Sc\, \kappa_n - \gamma ScK2,\ G_{3_{\kappa_n}} = -\gamma Sch_n' - \gamma\, Sc\, Sq,$

$G_{3_{\kappa_n'}} = \gamma Sc\, h_n - \frac{1}{2}\gamma ScS_q\varepsilon,\quad G_{3_{\kappa_n''}} = 1,\quad G_{3_\gamma} = Sc(h_n\kappa_n' - \kappa_n h_n') - ScSq(K2 + \kappa_n) - Sc\left(\frac{1}{2}Sq\varepsilon\kappa_n' + K2h_n'\right)$

(26)

Substituting Eq. (26) into Eq (23), Eq. (24), and Eq (25) in the derivatives that contain it, we get

$$(h_c'''')_n = -\frac{1}{\gamma}\, h_n'''' + hh_n''' - h_n'h_n'' - \frac{1}{2}S_q(3h_n'' - \varepsilon\, h_n''') - \frac{1}{Da}h_n'' \quad (27)$$

$$(\chi_c'')_n = -\frac{1}{\gamma}\,\chi_n'' + Pr(h_n\chi_n' - \chi_n h_n') - PrSq(K1 + \chi_n) - Pr\left(\frac{1}{2}S_q\varepsilon\chi_n' + K1h_n'\right), \quad (28)$$

$$(\kappa_c'')_n = -\frac{1}{\gamma}\,\kappa_n'' + Sc(h_n\kappa_n' - \kappa_n h_n') - ScSq(K2 + \kappa_n) - Sc\left(\frac{1}{2}Sq\varepsilon\kappa_n' + K2h_n'\right), \quad (29)$$

assume that the following initial condition

$$h_o(\varepsilon) = \Delta_{1o} + \Delta_{11}\varepsilon + \frac{\Delta_{12}}{2!}\varepsilon^2 + \frac{\Delta_{13}}{3!}\varepsilon^3, \quad (30)$$

$$\chi_o(\varepsilon) = \Delta_{20} + \Delta_{21}\varepsilon \quad (31)$$

$$\kappa_o(\varepsilon) = \Delta_{30} + \Delta_{31}\varepsilon \quad (32)$$

where

$h(0) = \Delta_{1o},\ \frac{dh(0)}{d\varepsilon} = \Delta_{11},\quad \frac{d^2h(0)}{d\varepsilon^2} = \Delta_{12},\ \frac{d^3h(0)}{d\varepsilon^3} = \Delta_{13}, \chi(0) = \Delta_{20},\ \frac{d\chi(0)}{d\varepsilon} = \Delta_{21},\ \kappa(0) = \Delta_{30}, \frac{d\kappa(0)}{d\varepsilon} = \Delta_{31}.$

From the boundary conditions of Equation (15),

$h_o(\varepsilon) = \varepsilon + (\varepsilon S_1 + \frac{\varepsilon^2}{2})\Delta_{12} + \frac{\varepsilon^3}{6}\Delta_{13},\ \ \chi_o(\varepsilon) = 1 - \varepsilon + (S_2 + \varepsilon)\Delta_{21},\ \ \kappa_o(\varepsilon) = 1 - \varepsilon + (S_3 + \varepsilon)\Delta_{31}$ (33)

The prerequisite condition for solving the problem using Δ_{11}, Δ_{12}, Δ_{21} and Δ_{31} are unknown. The analytical approximate solutions of Equations (12)-(14) at ($\varepsilon = 1$) may be used to derive the values of $\Delta_{11}, \Delta_{12}, \Delta_{21}$ and Δ_{31}. The iteration approach is used to produce the analytical approximations of the following equations:

$h1 = (1 + \Delta_{12}S_1)\varepsilon + 0.5\Delta_{12}\varepsilon^2 + 0.1666666667\Delta_{12}\varepsilon^3 + (0.041666666668\,(S_1\,\Delta_{12}^2 + \Delta_{12}) + 0.0625\,\Delta_{12}Sq + \frac{0.041666666668}{Da}\Delta_{12})\,\varepsilon^4 + (0.008333333334\Delta_{12}^2 + 0.01666666667Sq\,\Delta_{13} + \frac{0.008333333334\Delta_{13}}{Da})\varepsilon^5 + 0.002777777778\,\Delta_{12}\Delta_{13}\varepsilon^6 + 0.0003968253968\,\Delta_{13}^2\,\varepsilon^7.$

$\chi_1 = 1 - K1 + S_2\Delta_{21} + \Delta_{21}\,\varepsilon + (0.5\,\Delta_{12}\Delta_{21}S_1S_2\,Pr + 0.5\,\Delta_{21}\,S_2Pr + 0.5\Delta_{12\,S_1}Pr + 0.5\,Pr + 0.5S_2\Delta_{21}\,Sq\,\mathrm{Pr} + 0.5\,Sq\,\mathrm{Pr})\,\varepsilon^2 + (0.1666666666\Delta_{12}\Delta_{21}S_2\,Pr + 0.1666666666\,\Delta_{12}\,Pr + 0.25\,\Delta_{21}\,SqPr)\varepsilon^3 + (0.04166666665(\Delta_{12}\Delta_{21}\,Pr + \Delta_{13}\Delta_{21}S_2\,Pr + \Delta_{13}\,\mathrm{Pr}) + 2.5\times10^{-11}\,K1Pr\Delta_{13})\varepsilon^4 + 0.01666666667Pr\Delta_{13}\Delta_{21}\varepsilon^5.$

$\kappa_1 = 1 - K2 + S_3\Delta_{31} + \Delta_{31}\,\varepsilon + (0.5(S_3\Delta_{31} - K2 + 1)(S_1\Delta_{12} + 1)Sc + 0.5(\Delta_{31}S_3 + 1)Sq\,Sc) + 0.5ScK1(S_1\Delta_{12} + 1)\varepsilon^2 + (0.16666666666\Delta_{12}Sc(S_3\Delta_{31} - K2 + 1) + 0.1666666666\Delta_{31}\,ScSq + 0.1666666666\,Sc(0.5\Delta_{31}Sq + K2\Delta_{12}))\varepsilon^3 + (-0.08333333332(Sc - 0.5\Delta_{12}\Delta_{31})$

$$-0.5\Delta_{13}(S_3\Delta_{31} - K2 + 1) + 0.04166666668\Delta_{13}\,K2Sc)\varepsilon^4 + 0.01666666667\Delta_{13}\Delta_{31}Sc\varepsilon^5.$$

⋮

4. The Results of the Tabular

In this section, we examine in the influences of the flow parameter like squeezing parameter Sq, Darcy number Da, thermal stratification parameter $K1$, velocity slip parameter S_1, thermal slip parameter S_2, solutal slip parameter S_3, solutal stratification parameter $K2$, Schmidt number Sc, solutal stratification parameter, and Prandtl number Pr and Schmidt number Sc on the axial velocity $h(\varepsilon)$, and the radial velocity $h'(\varepsilon)$, temperature distribution $\chi(\varepsilon)$ and concentration distribution $\kappa(\varepsilon)$. Tables (1) - (4) present calculations of the convergence of values $\Delta_{11}, \Delta_{12}, \Delta_{13}, \Delta_{20}, \Delta_{21}, \Delta_{30}$ and Δ_{31} for different values of the emerging parameters. Tables (5)-(7) indicate the comparison of the obtained results PIT and the numerical results RK4^{M}. These tables show outline that the results are a good match to the numerical solution produced by RK4^{M}.

Table.1: The computed values of Δ_{11}, Δ_{12}, Δ_{13}, Δ_{20},Δ_{21},Δ_{30} and $\Delta_{31}$when S_1=S_2=S_3=0.1, Sq= -0.001, Da = 0.9, Pr = 0.2, Sc=0.1, K1=K2=0.1.

Approximation	Δ_{11}	Δ_{12}	Δ_{13}	Δ_{20}	Δ_{21}	Δ_{30}	Δ_{31}
Order1	0.70486738	-2.9513261	5.42109262	0.8162498614	-0.837501385	0.817217976	-0.827820234
Order2	0.70377638	-2.9622361	5.47506207	0.8165550956	-0.834449044	0.817367134	-0.826328658
Order3	0.70376113	-2.9623886	5.47568864	0.8165568436	-0.834431563	0.817368239	-0.826317603
Order4	0.70376107	-2.9623892	5.47569084	0.8165568455	-0.834431544	0.817368240	-0.826317593
Order5	0.70376107	-2.9623892	5.47569084	0.8165568455	-0.834431544	0.817368240	-0.826317593

Table.2: The computed values of Δ_{11}, Δ_{12}, Δ_{13}, Δ_{20},Δ_{21},Δ_{30} and $\Delta_{31}$when S_1=S_2=S_3=0, Sq = 0.01, Da = 0.7, Pr = 0.6, Sc=0.5, K1=K2=0.

Approximation	Δ_{11}	Δ_{12}	Δ_{13}	Δ_{20}	Δ_{21}	Δ_{30}	Δ_{31}
Order1	1.0000000	-2.928246031	5.368620778	1.0000000	-0.8379589547	1.0000000	-0.8280488461
Order2	1.0000000	-2.939088184	5.422261919	1.0000000	-0.8349160042	1.0000000	-0.8265625753
Order3	1.0000000	-2.939233676	5.422858038	1.0000000	-0.8348991588	1.0000000	-0.8265517414
Order4	1.0000000	-2.939234148	5.422859821	1.0000000	-0.8348991466	1.0000000	-0.8265517350
Order5	1.0000000	-2.939234148	5.422859821	1.0000000	-0.8348991466	1.0000000	-0.8265517350

Table.3: The computed values of Δ_{11}, Δ_{12}, Δ_{13}, Δ_{20}, Δ_{21}, Δ_{30} and $\Delta_{31}$when S_1=S_2=S_3=1, Sq= 0.05, Da=1, Pr = 0.7, Sc=0.5, K1=K2=1.

Approximation	Δ_{11}	Δ_{12}	Δ_{13}	Δ_{20}	Δ_{21}	Δ_{30}	Δ_{31}
Order1	-1.970199599	-2.970199599	5.463948286	-0.837126940	-0.8371269397	-0.827633164	-0.8276331643
Order2	-1.981163731	-2.981163731	5.518180448	-0.834066955	-0.8340669549	-0.826126052	-0.8261372878
Order3	-1.981322115	-2.981322115	5.518832089	-0.834048954	-0.8340489541	-0.826126052	-0.8261260521
Order4	-1.981322784	-2.981322784	5.518834651	-0.834048929	-0.8340489293	-0.826126039	-0.8261260393
Order5	-1.981322784	-2.981322784	5.518834651	-0.834048929	-0.8340489293	-0.826126039	-0.8261260393

Table.4: The computed values of Δ_{11}, Δ_{12}, Δ_{13}, $\Delta_{20}, \Delta_{21}, \Delta_{30}$ and $\Delta_{31}$when S_1=0.1, S_2=0.2, S_3=0.3, Sq = 0.05, Da =1,2, Pr = 0.3, Sc=0.1, K1=0.1, K2=0.2.

Approximation	Δ_{11}	Δ_{12}	Δ_{13}	Δ_{20}	Δ_{21}	Δ_{30}	Δ_{31}
Order1	0.715579961	-2.84420038	5.17695241	0.73207559	-0.8396220352	0.5513360371	-0.82887987
Order2	0.714521775	-2.85478224	5.22933403	0.73267726	-0.8366136908	0.5517759893	-0.82741336
Order3	0.714509746	-2.85490253	5.22982149	0.73268017	-0.8365991445	0.5517789985	-0.82740333
Order4	0.714509731	-2.85490268	5.22982200	0.73268016	-0.8365991549	0.5517789969	-0.82740334
Order5	0.714509731	-2.85490268	5.22982200	0.73268016	-0.8365991549	0.5517789969	-0.82740334

Table5: The Outcome values of $h(\varepsilon), \chi(\varepsilon), \kappa(\varepsilon)$ for PIT and RK4^{M} when S_1=S_2=S_3=0.1, Sq= -0.001, Da = 0.9, Pr = 0.2, Sc=0.1, K1=K2=0.1.

ε	h(ε)	RK4^{M}	Percentage error	χ (ε)	RK4^{M}	Percentage error
0.0	0.0000000000	0.00000000000	0.00000000	0.8165550956	0.8165550956	0.00000000
0.1	0.0564577770	0.05645658648	2.1×10^{-5}	0.7336698147	0.7338845500	2.9×10^{-4}
0.2	0.0884892187	0.08848709969	2.3×10^{-5}	0.6516100696	0.6519606823	5.4×10^{-4}
0.3	0.1009257250	0.10092286140	2.8×10^{-5}	0.5700247852	0.5704529894	7.5×10^{-4}
0.4	0.0982946707	0.09829119226	3.5×10^{-5}	0.4886656458	0.4891301995	9.5×10^{-4}
0.5	0.0849029714	0.08489897838	4.6×10^{-5}	0.4073685471	0.4082263699	1.1×10^{-3}
0.6	0.0649042172	0.06489978828	6.7×10^{-5}	0.3260370995	0.3265034736	1.4×10^{-3}
0.7	0.0423543099	0.04234941597	1.1×10^{-4}	0.2446276765	0.2450789408	1.8×10^{-3}
0.8	0.0212601520	0.02125427589	2.6×10^{-4}	0.1631355495	0.1633814744	1.5×10^{-3}
0.9	0.0056257364	0.00561676299	2.1×10^{-5}	0.0815817150	0.0816931969	1.3×10^{-3}
1.0	-0.000500000	0.00050000000	0.00000000	0.0000000000	0.0000000000	0.00000000

Table 6: The Outcome values of h(ε), χ(ε) for PIT and RK4^{M} when S_1=S_2=S_3=0.1, Sq= 0.001, Da = 0.9, Pr = 0.2, Sc=0.1, K1=K2=0.1.

ε	h(ε)	RK4^{M}	Percentage error	$\chi(\varepsilon)$	RK4^{M}	Percentage error
0.0	0.00000000000	0.00000000000	0.0000000	0.8165373717	0.8165373717	
0.1	0.05651818545	0.05651699571	2.1×10^{-5}	0.7336366004	0.7338520689	0.00000000
0.2	0.08864302264	0.08864090511	2.3×10^{-5}	0.6515659100	0.6519180179	2.9×10^{-4}
0.3	0.10119741460	0.10119455310	2.8×10^{-5}	0.5699742032	0.5704046618	5.4×10^{-4}
0.4	0.09869987362	0.09869639785	3.5×10^{-5}	0.4886129727	0.4890805081	7.5×10^{-4}
0.5	0.08544810007	0.08544410973	4.6×10^{-5}	0.4073177755	0.4077950118	9.5×10^{-4}
0.6	0.06558615691	0.06558172942	6.7×10^{-5}	0.3259917636	0.3264623721	1.1×10^{-3}
0.7	0.04316016796	0.04315526801	1.1×10^{-4}	0.2445907585	0.2450467331	1.4×10^{-3}
0.8	0.02216706943	0.02216116169	2.6×10^{-4}	0.1631094206	0.1633710756	1.8×10^{-3}
0.9	0.00660076029	0.00659168104	1.3×10^{-3}	0.0815681050	0.0819905105	1.0×10^{-3}
1.0	0.00050000000	0.00050000000	0.00000000	0.0000000000	0.0000000000	5.1×10^{-3}
						0.00000000

Table 7: The Outcome values of $\kappa(\varepsilon)$ for PIT and RK4^{M} when S_1=S_2=S_3=0.1, Da = 0.9, Pr = 0.2, Sc=0.1, K1=K2=0.1.

	Sq= 0.001			Sq= -0.001		
ε	$\kappa(\varepsilon)$	RK4^{M}	Percentage error	κ(ε)	RK4^{M}	Percentage error
0.0	0.8173582569	0.8173582569	0.0000000	0.8173671342	0.8173671342	0.0000000000
0.1	0.7349977002	0.7349977193	2.5×10^{-8}	0.7350143338	0.7350143530	2.8×10^{-8}
0.2	0.6530526135	0.6530526378	3.7×10^{-8}	0.6530747240	0.6530747481	3.6×10^{-8}
0.3	0.5713473607	0.5713473769	2.8×10^{-8}	0.5713726810	0.5713726970	2.8×10^{-8}
0.4	0.4897576122	0.4897575964	3.2×10^{-8}	0.4897839733	0.4897839578	3.1×10^{-8}
0.5	0.4082010802	0.4082009637	2.8×10^{-7}	0.4082264843	0.4082263699	2.8×10^{-7}
0.6	0.3266293016	0.3266288984	1.2×10^{-6}	0.3266519814	0.3266515858	1.2×10^{-6}
0.7	0.2450201834	0.2450190614	4.5×10^{-6}	0.2450386490	0.2450375460	4.5×10^{-6}
0.8	0.1633710756	0.1633683621	1.5×10^{-5}	0.1633841425	0.1633814744	1.6×10^{-5}
0.9	0.0816921656	0.0819905105	3.6×10^{-4}	0.0816989706	0.0816931969	7.0×10^{-5}
1.0	0.0000000000	0.0000000000	0.00000000	0.0000000000	0.000000000	0.00000000

5. Graph discussion of the plates moving each other ($Sq < 0$).

After obtaining the approximate analytical solutions for Equations (12) and (14) about the initial and boundary conditions of Equations (15) using Maple software, the basic purpose of this article is to demonstrate the behavior of important parameters relevant to the state mathematics problem when the plates move each other. The effects of these parameters completely have different attributes such as axial velocity $h(\varepsilon)$, radial velocity

$h'(\varepsilon)$, temperature $\chi(\varepsilon)$ and concentration $\kappa(\varepsilon)$. Figure (3) illustrates the squeezing parameter Sq influences the velocity components, temperature, and concentration. It can be seen from this figure an enlargement in velocity profiles (axial, redial) and the reduction of the temperature and concentration with increasing squeezing parameters. The physical explanation for this is the width of the gap between the plates will compress with an increase in the squeezing coefficient, therefore, greater compressive strength provides more fluid deformation. Hence, the velocity components are enhanced. Figure (4) explains the effect of increasing K1 and K2 on the temperature and concentration profiles, respectively. This figure shows that these distributions behave similarly and the curves are decreasing. Figure (5) discusses the influence of the S_1 on the axial and radial velocity. This figure plots the axial velocity become decreasing. While the radial is divided into two cases from $0 < \varepsilon \leq 3.5$ is decreasing and $3.5 < \varepsilon < 1$ is increasing. Figure (6) demonstrates the increase of S_2 and S_3 on the temperature and concentration profiles, respectively. From this figure, it can be seen that these profiles are decreasing. Figure (7) explains the effect of increasing Pr and Sc on the temperature and concentration profiles, respectively. This figure shows that these distributions behave similarly and the curves are increasing. Figures (8) and (9) indicate the counter of the stream function. These figures show that the stream function is in form of curves that are not intersecting with increasing the dimensional constant a and kinematics viscosity v. In fluid mechanics, the stream function can be defined by the path of imaginary particles suspended in and carried with a fluid. In steady flow, the streamlines are stationary but the fluid is in motion. Physically, the fluid velocity is relatively high, the streamline is combined. While they are opened when the fluid is relatively still.

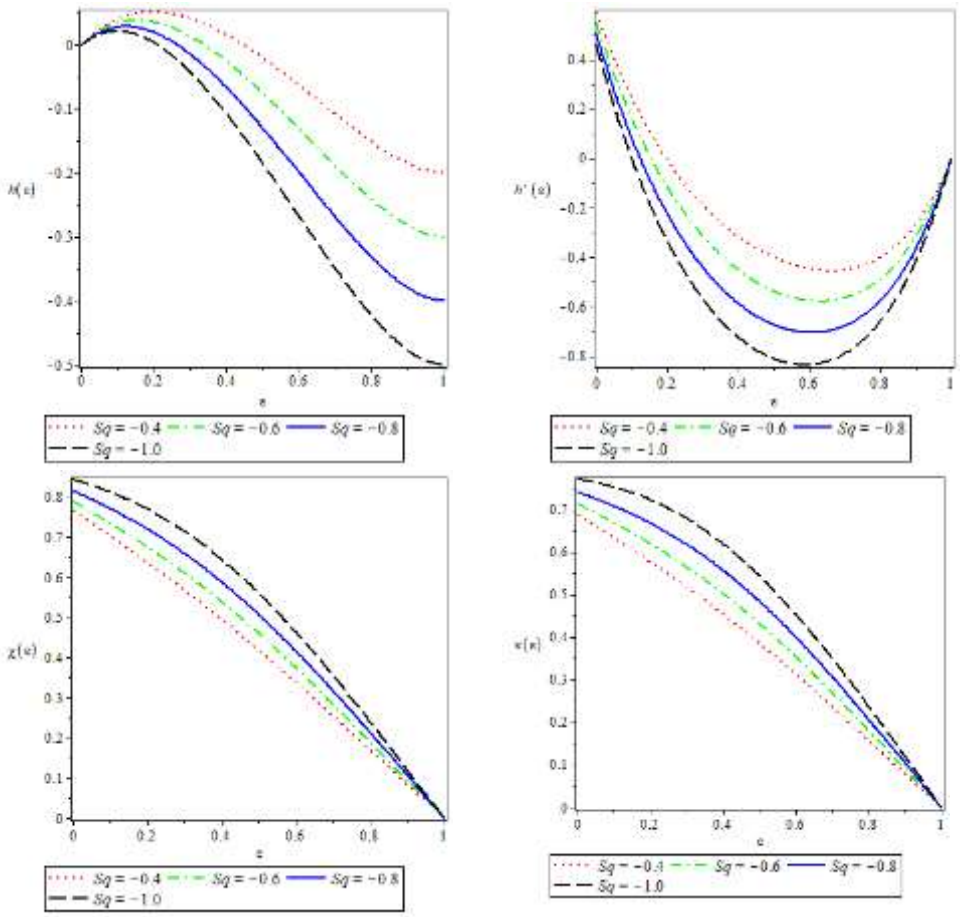

Figure.3: The behavior of $h(\varepsilon)$, $h'(\varepsilon)$, $\chi(\varepsilon)$ and $\kappa(\varepsilon)$ with various Sq for S_1=0.1, S_2=0.2, Da = 0.1, Pr = Sc=1.2, K1=0.1, K2=0.2.

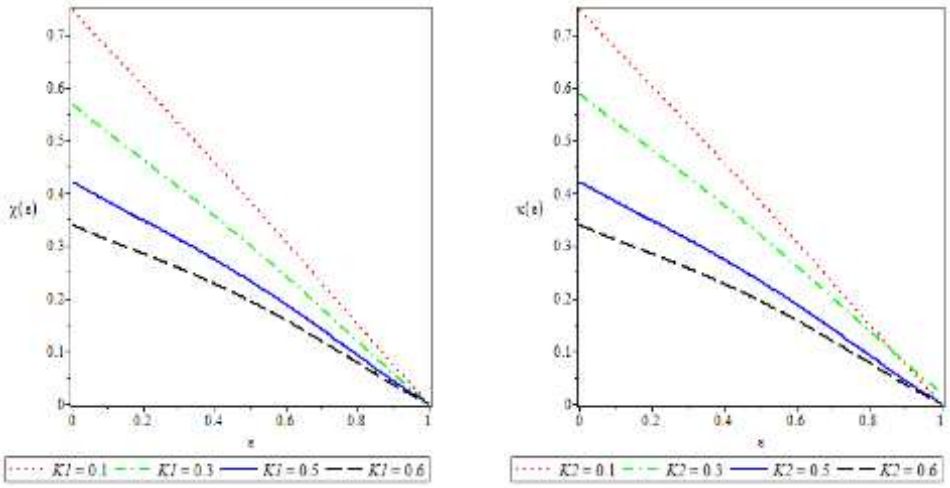

Figure 4: The behavior of $\chi(\varepsilon)$ and $\kappa(\varepsilon)$ with various K1 and K2 respectively, for S_1=0.1, S_2=0.2, Da = 0.1, Pr = Sc=1.2.

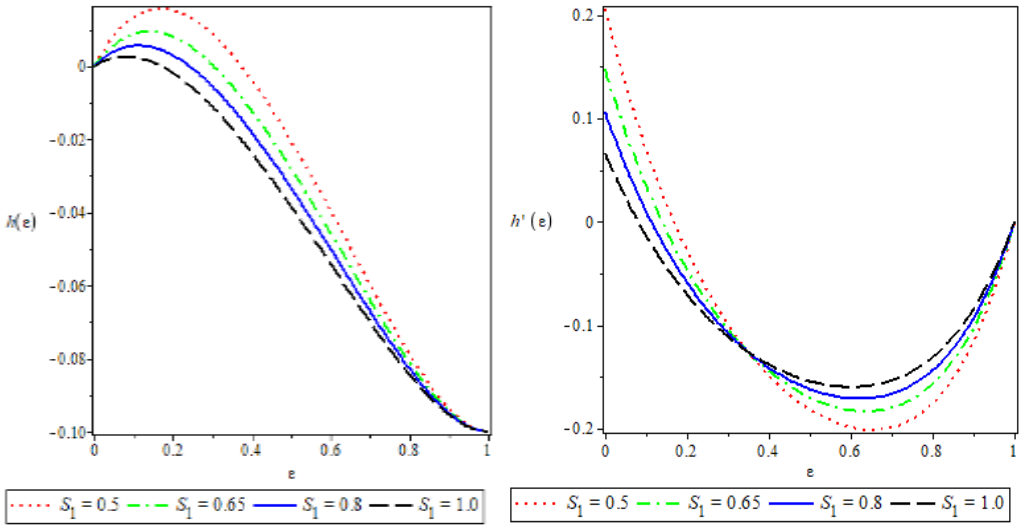

Figure 5: The behavior of $h(\varepsilon)$ and $h'(\varepsilon)$ with various S_1 for S_2=S_3=0.2, Sq= -0.2, Da = 0.1, Pr = Sc=1.2, K1=0.1, K2=0.2.

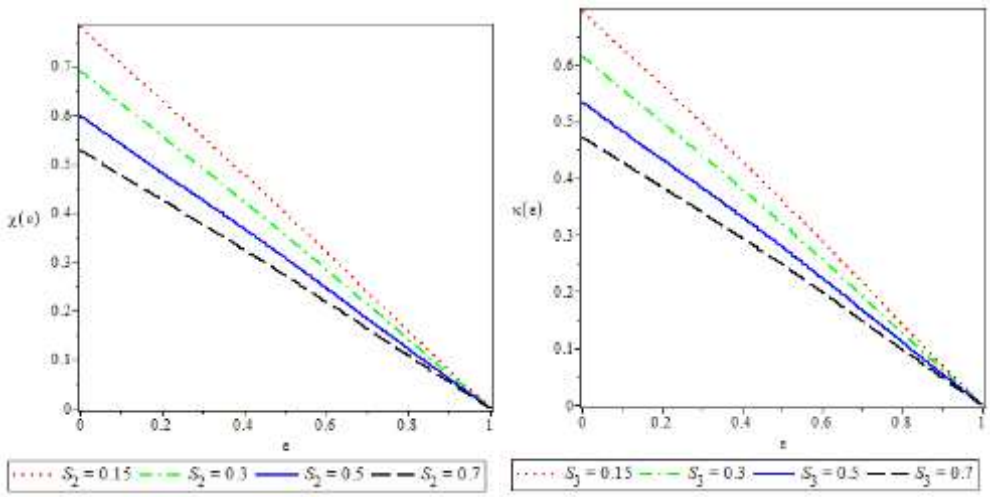

Figure 6: The behavior of $\chi(\varepsilon)$ and $\kappa(\varepsilon)$ with various S_2 and S_3 for S_1=0.1, Sq= -0.2, Da = 0.1, Pr = Sc=1.2, K1=0.1, K2=0.2.

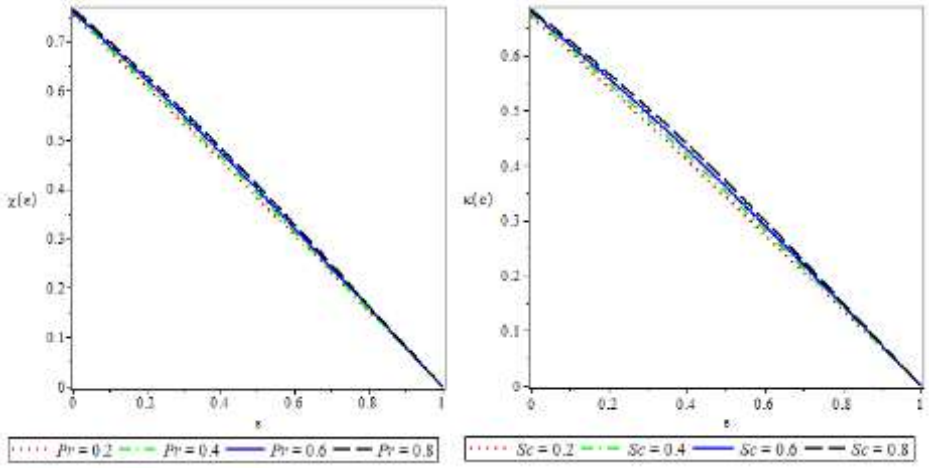

Figure.7: The behavior of $\chi(\varepsilon)$ and $\kappa(\varepsilon)$ with various Pr and Sc respectively, for S_1=0.1, $S_2 = S_3$=0.2, Da = 0.1, K1=0.1, K2=0.2.

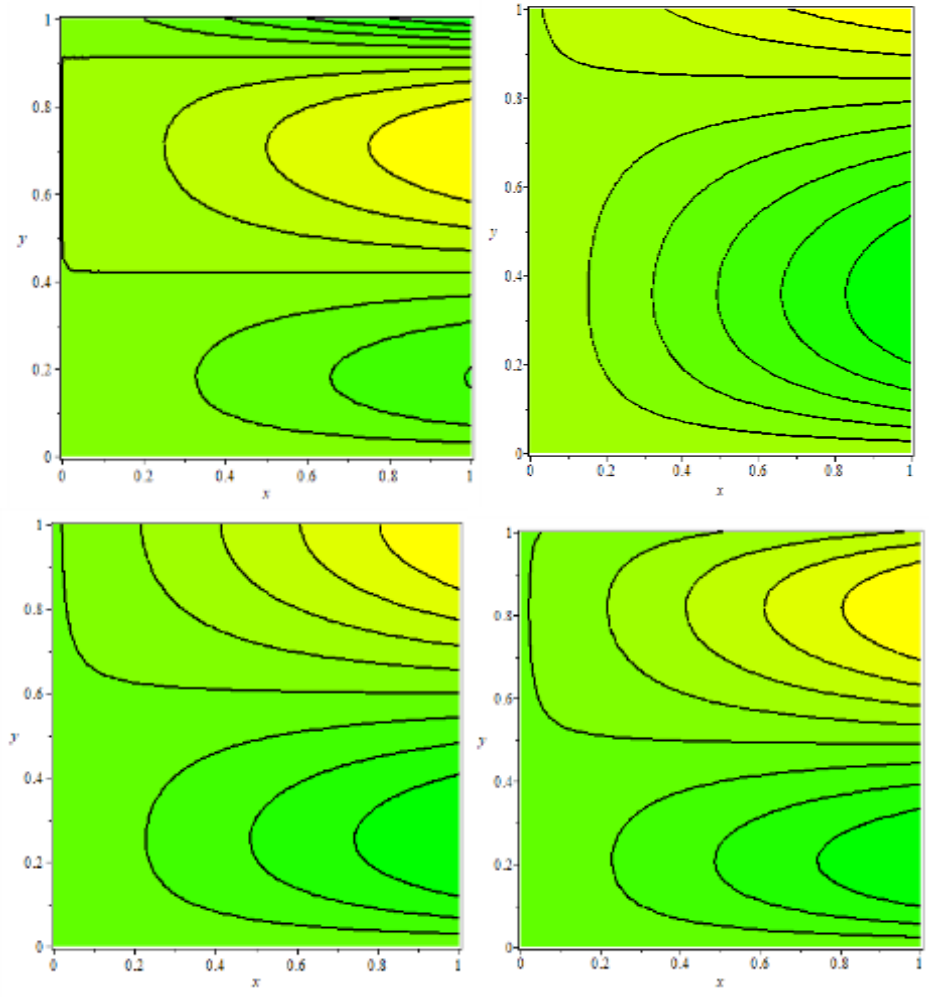

Figure.8: The behavior of the stream function for $S_1 = S_2 = S_3$ =0.1, Sq=-0.2, Pr = 0.2, Sc=K1=0.1, K2=0.1.

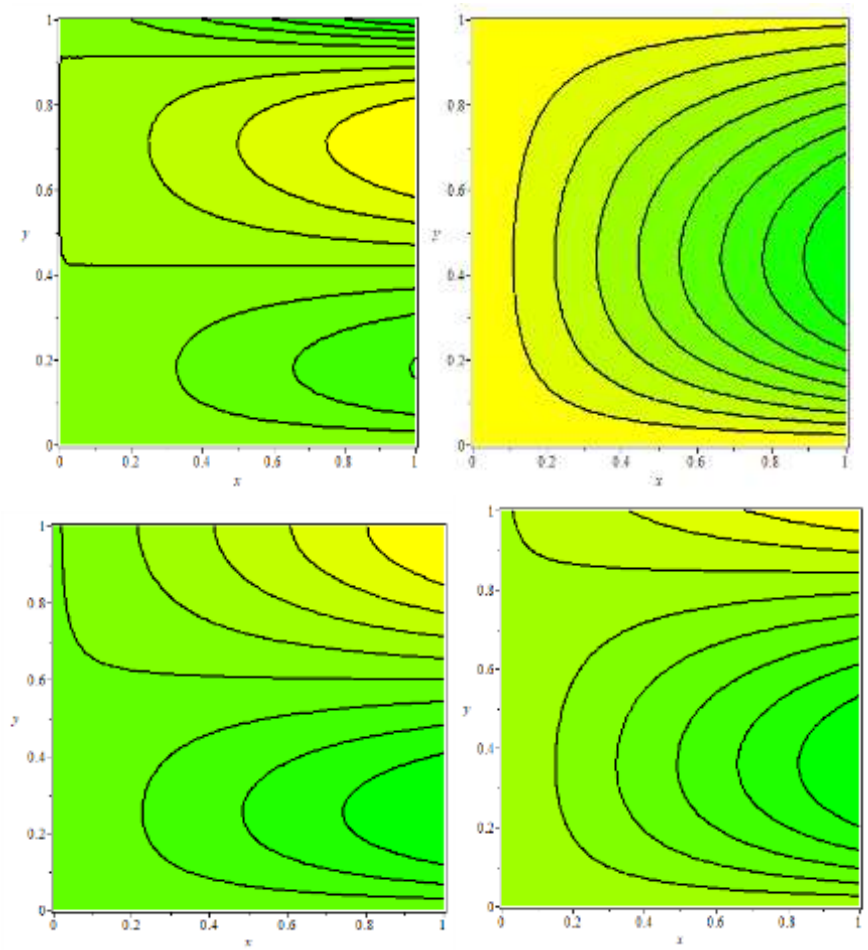

Figure.9. The behavior of the stream function for S_1= S_2=S_3 =0.1, Sq=-0.2, Pr = 0.2, Sc=K1=0.1, K2=0.1.

6. Discussion of the graphic of the plates moving away ($Sq > 0$).

The analytical solutions of the slip analysis to squeeze fluid flow when the plates move apart are simulated using the results graphs presented in Figures (10)-(17) under the aid of Maple software. The effect of S_1, S_2,S_3, Sq, K1, and K2 have the same behavior the plates moving each other whereas the effect of Pr and Sc are opposite for the behavior of the plates moving each other. The effect of D_a on axial and radial velocity is shown in Figure (11). This figure gives the axial velocity that is increment and the radial velocity is increasing for $0 < \varepsilon < 0.5$ with decreasing for $0.5 \leq \varepsilon < 1$. In Figures (16)-(17), the counters of stream function with increasing the dimensional constant a and kinematics viscosity v are investigated. These figures show that the lines are parallel and the intersection does not exist and the curves are more tortuosity when increasing a. However, the opposite can be noticed when the tortuosity decreases.

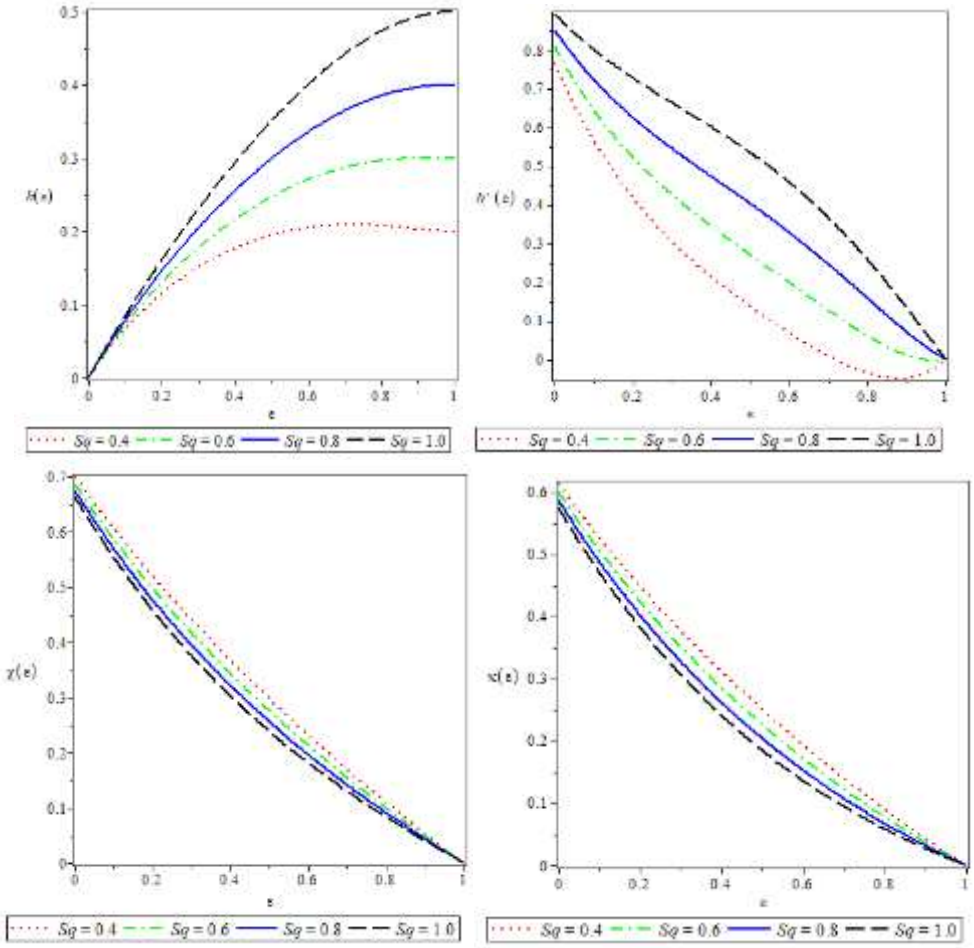

Figure 10: The behavior of $h(\varepsilon)$, $h'(\varepsilon)$, $\chi(\varepsilon)$ and $\kappa(\varepsilon)$ with various Sq for S_1=0.1, S_2=0.2, Da = 0.1, Pr = Sc=1.2, K1=0.1, K2=0.2.

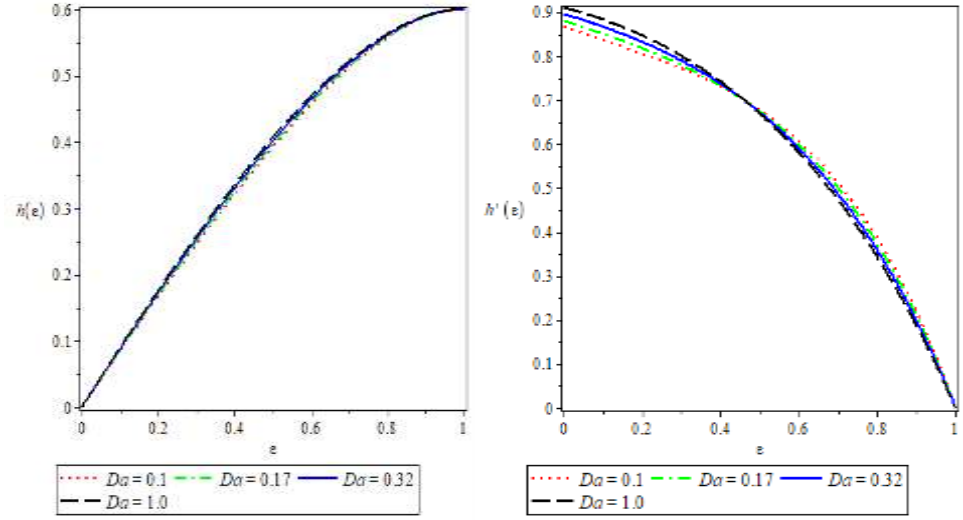

Figure. 11: The behavior of $h(\varepsilon)$ and $h'(\varepsilon)$ with various Da for S_1=0.4, S_2=0.2, Sq= Pr = Sc=1.2, K1=0.1, K2=0.2.

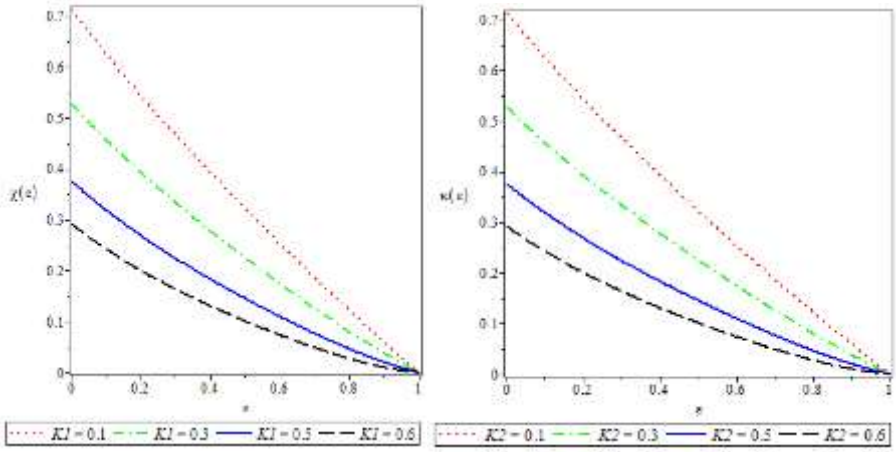

Figure 12: The behavior of $\chi(\varepsilon)$ and $\kappa(\varepsilon)$ with various K1 and K2, respectively for S_1=0.4, S_2=0.2, Sq= Pr = Sc=1.2 .

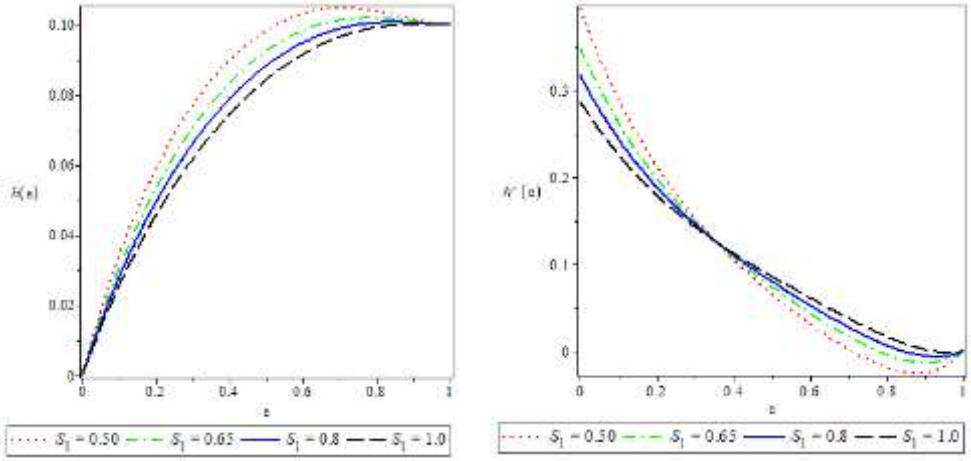

Figure 13: The behavior of $h(\varepsilon)$ and $h'(\varepsilon)$ with various S_1 for $S_2 = 0.2$ Sq= Pr = Sc=1.2, K1=0.1, K2=0.2.

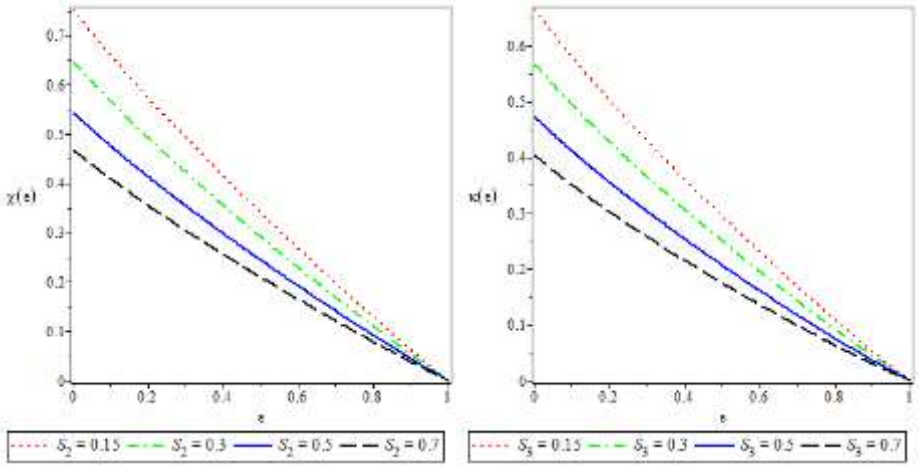

Figure 14: The behavior of $\chi(\varepsilon)$ and $\kappa(\varepsilon)$ with various S_2 and S_3 respectively for S_1= 0.4, Sq= Pr = Sc=1.2, K1=0.1, K2=0.2.

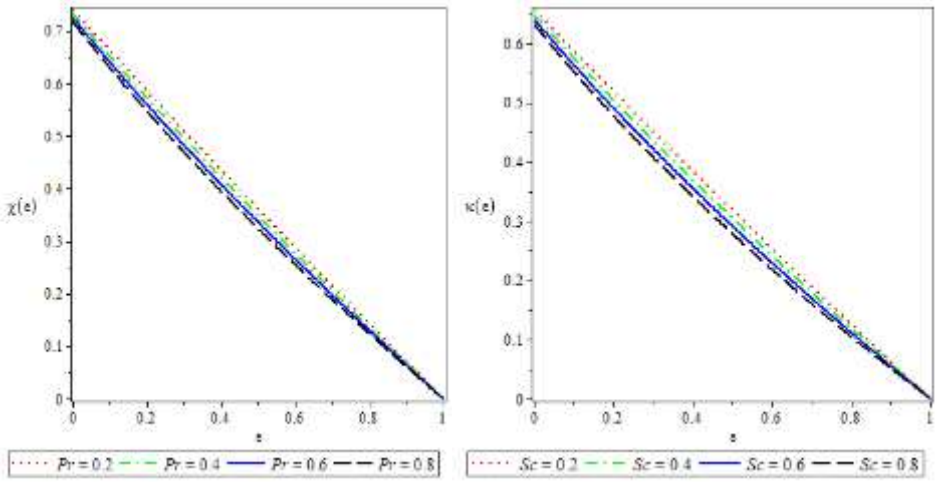

Figure 15: The behavior of $\chi(\varepsilon)$ and $\kappa(\varepsilon)$ with various Pr and Sc respectively for S_1=0.4, $S_2 = 0.2, S_3 = 0.2$, K1=0.1, K2=0.2.

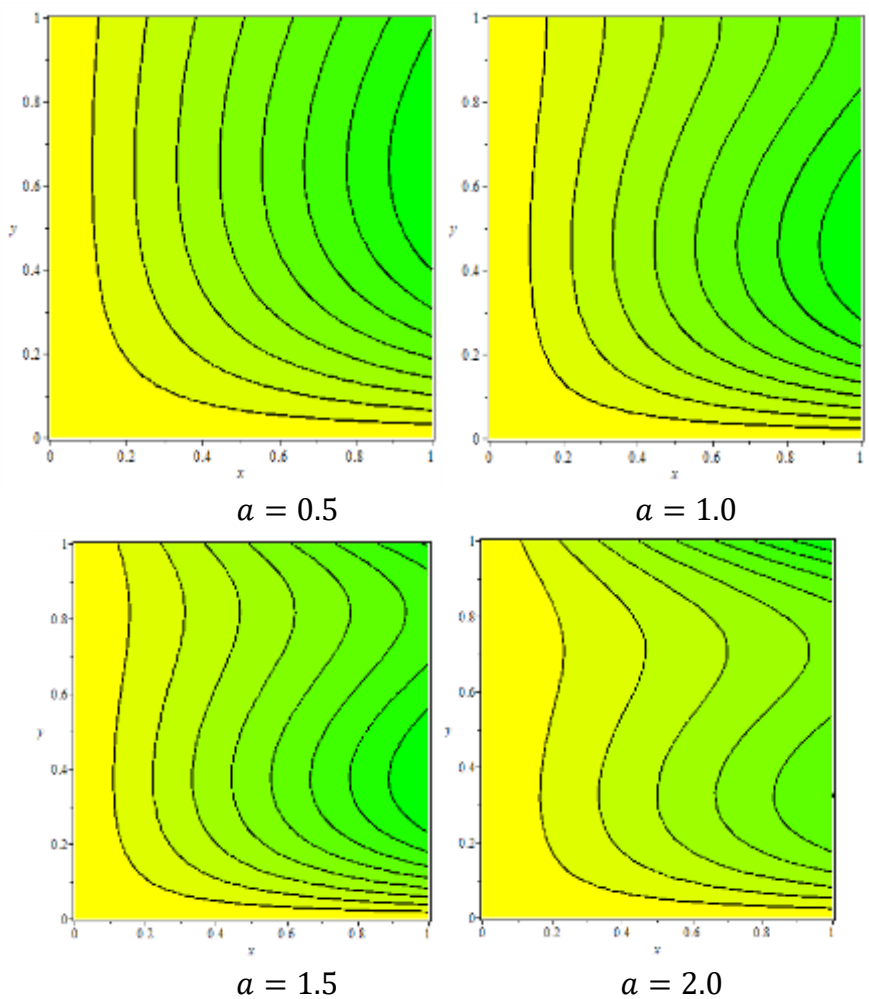

Figure 16: The behavior of the stream function for S_1= S_2=S_3 =0.1, Sq= Pr = 0.2, Sc= K1=0.1, K2=0.1.

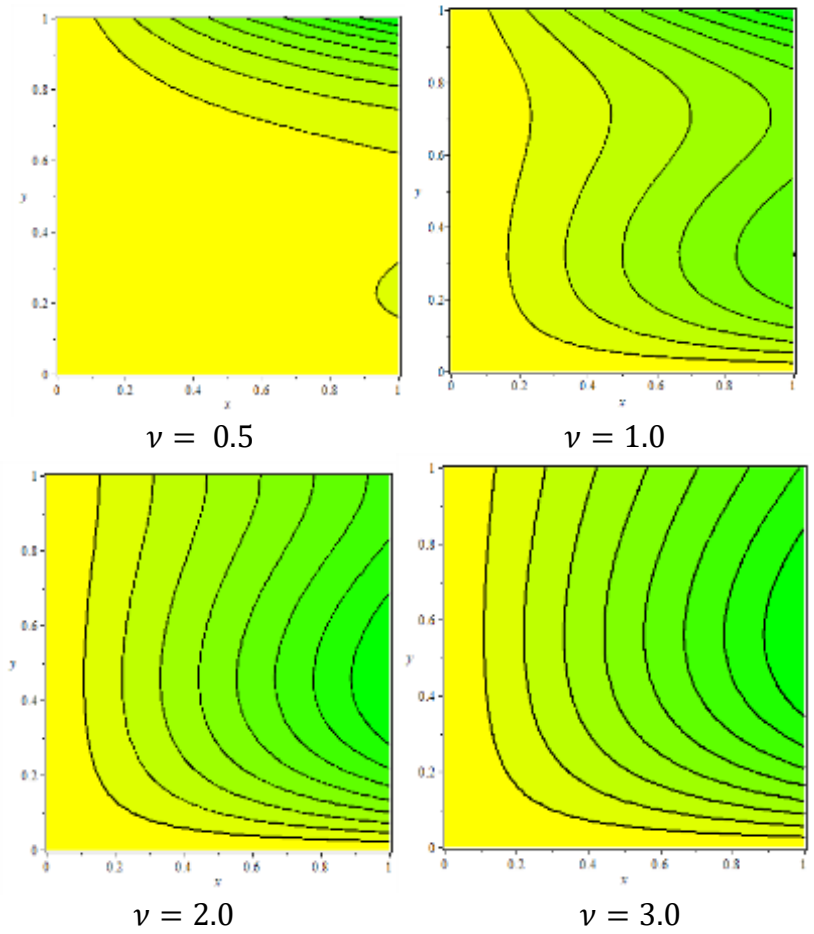

Figure 17: The behavior of the stream function for S_1= S_2=S_3 =0.1, Sq= Pr = 0.2, Sc= K1=0.1, K2=0.1.

7. Graphic discussions of physical quantities

In Figures (18)-(23), we depict interpretations of the impacts of factors on physical variables including coefficient of skin friction, Nusselt number, and Sherwood number. Skin friction coefficient, Nusselt number, and Sherwood number are depicted for various values of the velocity parameter slip S_1, thermal parameter slips S_2, and singular slip parameter S_3 in Figure (18). Every quantity is shown to decrease in this figure.

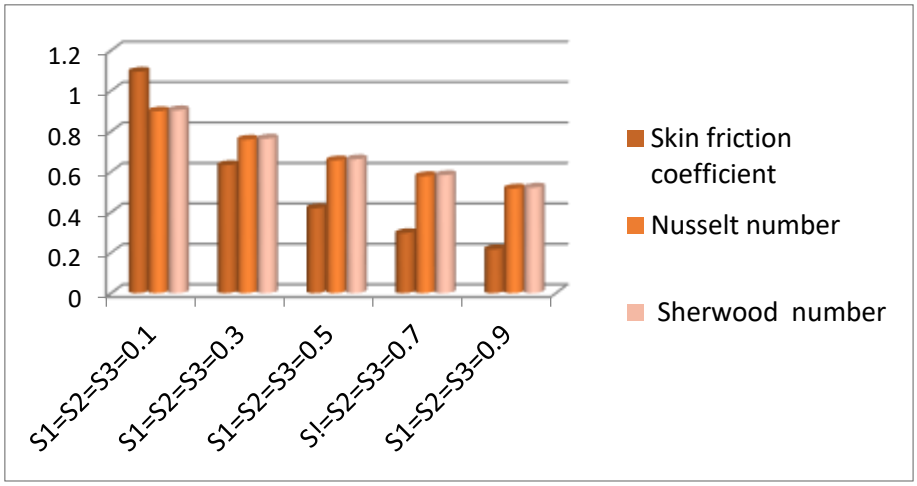

Figure 18. The behavior of the Skin friction coefficient, Nusselt number, and Sherwood number for various S_1, S_2 and S_3.

Figure (19) shows how the Nusselt number and Sherwood number are affected by various val ues of the thermal stratification parameter $K1$ and the solutal stratification parameter $K2$, resp ectively. This figure demonstrates Nusselt number is reduced for an increase $K1$, the behavior of the Sherwood number is similar for the Nusselt number with an increase $K2$.

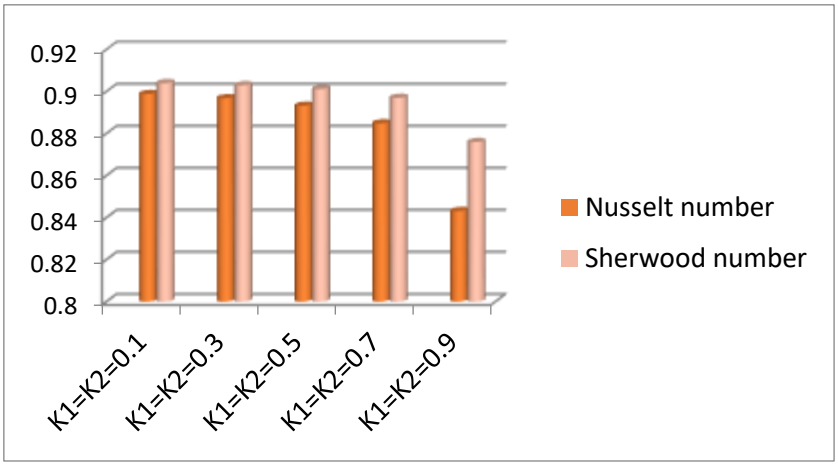

Figure 19: The behavior of the Nusselt number and Sherwood number for various $K1$ and $K2$.

Figure (20) and Figure (21) indicted the effects of the three quantities plotted for sundry values of squeezing number Sq. These figures show these quantities decrease as the emerging squeezing parameter increase.

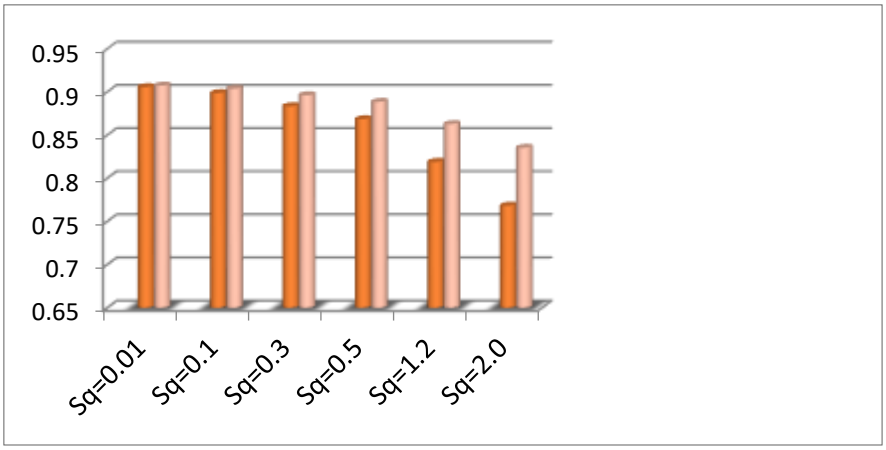

Figure 20: The behaviorof the Sherwood number and the Nusselt number for different Sq.

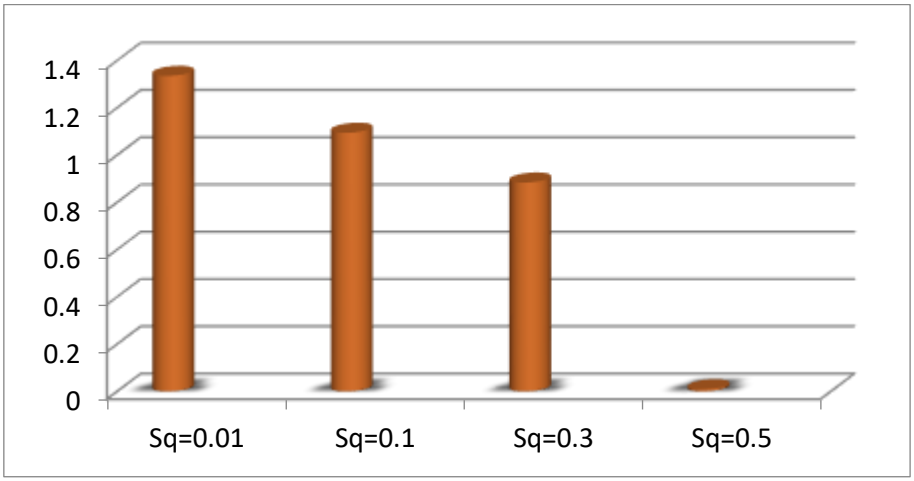

Figure.21: The Skin friction coefficient's behavior for different Sq.

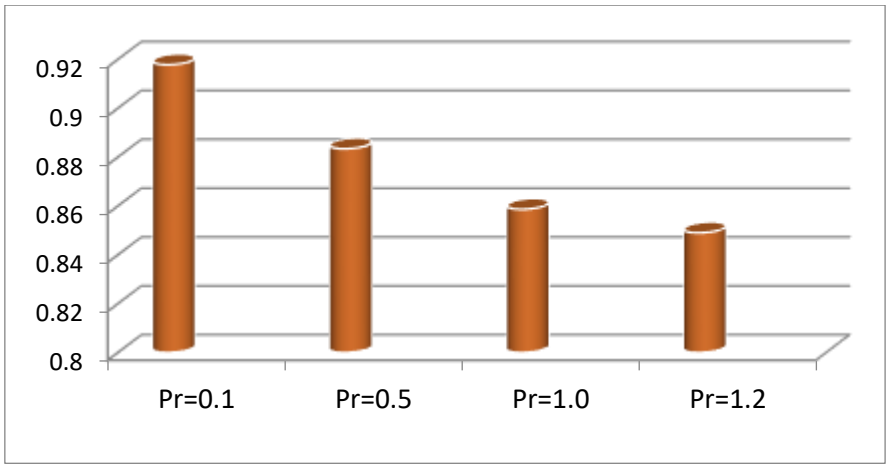

Figure 22: The behavior of Nusselt number for various Pr.

Figure (22) shows the Nusselt number for various Prandtl number Pr values. The behavior of the Sherwood number for various values of the Schmidt parameter Sc was described in Figure (23). These Figures demonstrate that an increase causes the Nusselt number to decrease, whereas an increase in Sc causes the Sherwood number to grow.

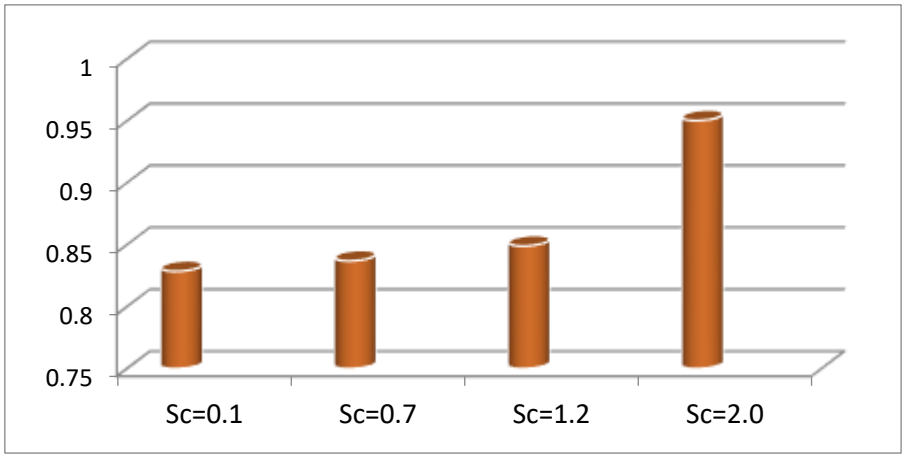

Figure 23: The Sherwood number's behavior for different Sc.

8. The Discussions of convergence analysis

In this part, the implementation of the theorems in [18], [19] is to analyze the convergence of the solutions of PIT. If there exists $0 < \varpi_{ki} < 1$ then $\left\|\overline{\Pi}_{k(i+1)}\right\| \leq \varpi_{ki} \left\|\overline{\Pi}_{ki}\right\|, k = 1,2,3, i = 0,1,2, \ldots$, is the condition of convergent. which

$\overline{\Pi}_{10} = h_0,$
$\overline{\Pi}_{20} = \chi_0,$
$\overline{\Pi}_{30} = \kappa_0,$
$\overline{\Pi}_{10} + \overline{\Pi}_{11} = h_0 + (h_c)_0,$
$\overline{\Pi}_{20} + \overline{\Pi}_{21} = \chi_0 + (\chi_c)_0,$
$\overline{\Pi}_{30} + \overline{\Pi}_{31} = \kappa_0 + (\kappa_c)_0,$
$\overline{\Pi}_{10} + \overline{\Pi}_{11} + \overline{\Pi}_{12} = h_0 + (h_c)_0 + (h_c)_1,$
$\overline{\Pi}_{20} + \overline{\Pi}_{21} + \overline{\Pi}_{22} = \chi_0 + (\chi_c)_0 + (\chi_c)_1,$
$\overline{\Pi}_{30} + \overline{\Pi}_{31} + \overline{\Pi}_{32} = \kappa_0 + (\kappa_c)_0 + (\kappa_c)_1$
$\vdots$
$\overline{\Pi}_{10} + \overline{\Pi}_{11} + \overline{\Pi}_{12} + \cdots + \overline{\Pi}_{1n} = h_0 + (h_c)_0 + (h_c)_1 + \cdots + (h_c)_n,$

$\overline{\Pi}_{20} + \overline{\Pi}_{21} + \overline{\Pi}_{22} + \cdots + \overline{\Pi}_{2n} = \chi_0 + (\chi_c)_0 + (\chi_c)_1 + \cdots + (\chi_c)_n,$
$\overline{\Pi}_{30} + \overline{\Pi}_{31} + \overline{\Pi}_{32} + \cdots + \overline{\Pi}_{3n} = \kappa_0 + (\kappa_c)_0 + (\kappa_c)_1 + \cdots + (\kappa_c)_n,$
All solutions are achieved for the condition of convergent in Tables. (8) – (10) as follows:

Table.8: The values of convergence for S_1=S_2=S_3=0.1, Da = 0.9, Pr = 0.2, Sc=0.9, K1=K2=0.2.

$\varpi_{1i_{\|\cdot\|_\infty}}$	$Sq = 0.1$	$Sq = -0.1$	$Sq = 0.01$	$Sq = -0.01$	$Sq = 0.05$	$Sq = -0.05$
ϖ_{10}	0.1656029283	0.1371020578	0.1527741499	0.1499240140	0.1584752186	0.1442245977
ϖ_{11}	0.0211662361	0.0072358045	0.0142977474	0.01277113521	0.0173506533	0.0097175683
⋮	⋮	⋮	⋮	⋮	⋮	⋮

Table.9: The values of convergence for S_1=S_2=S_3=0.1, Da = 0.9, Pr = 0.2, Sc=0.9, K1=K2=0.2.

$\varpi_{2i_{\|\cdot\|_\infty}}$	$Sq = 0.1$	$Sq = -0.1$	$Sq = 0.01$	$Sq = -0.01$	$Sq = 0.05$	$Sq = -0.05$
ϖ_{20}	0.1031884255	0.1216908328	0.1108241111	0.1126633413	0.1073068890	0.1165163177
ϖ_{21}	0.0830810792	0.0693073494	0.0773932718	0.0760122189	0.0800299166	0.0731291133
⋮	⋮	⋮	⋮	⋮	⋮	⋮

Table.10: The values of convergence for S_1=S_2=S_3=0.1, Da = 0.9, Pr = 0.2, Sc=0.9, K1=K2=0.2.

$\varpi_{3i_{\|\cdot\|_\infty}}$	$Sq = 0.1$	$Sq = -0.1$	$Sq = 0.01$	$Sq = -0.01$	$Sq = 0.05$	$Sq = -0.05$
ϖ_{20}	0.4622006152	0.5444755073	0.4950895366	0.5032491413	0.4797348925	0.5206147798
ϖ_{21}	0.0404236483	0.0693073494	0.0376962965	0.0381217881	0.0364102767	0.0385473894
⋮	⋮	⋮	⋮	⋮	⋮	⋮

Consequently, the series of approximate- analytical solutions $h(\varepsilon)$, $\chi(\varepsilon)$ and $\kappa(\varepsilon)$ obtained by PIT can that say is convergent.

9. Conclusion

In this article, the designation of the slip analysis for squeezing flow between parallel plates model is solved to establish the analytical expressions for concentration, temperature, and velocity by using PIT with the help of similarity transform. It can be seen that PIT is successfully implemented for slip analysis of squeezing flow among parallel plates to find a new approximate analytical solution. The obtained results for these distributions are plotted to see the impact of parameters graphically. As a result, the fluid velocity exhibits the larger variance of the cross-flow slip velocity parameter in that direction. The function of the thermal stratification and slip parameters is reduced by the temperature field. For the solutal stratification parameter and solutal slip parameter, the fluid concentration decreases. Also, the Nusselt number and the Sherwood number decrease as all proposed parameters increase except for the Schmidt parameter when it is increased leading to increase physical quantities.

References

[1] C. Navier, "Memorie sur les lois du lois du mouvement des fluids, Mem," *Acad Sci Inst France,* vol. 6, pp. 298-440, 1827.

[2] J. Maxwell, "On stresses in rarefied gases arising from inequalities of temperature," *Philosophical Transactions of the royal society of London,* vol. 170, pp. 231-256, 1879.

[3] I. Rao, and K. R. Rajagopal, "The effect of the slip boundary condition on the flow of fluids in a channe," *Acta Mechanica,* vol. 135, pp. 113-126, 1999.

[4] T. Hayat, M. Farooq, and A. Alsaedi, "Thermally stratified stagnation point flow of Casson fluid with slip conditions," *International Journal of Numerical Methods for Heat & Fluid Flow,* vol. 25, no. 4, pp. 724-748, 2015.

[5] A. M. Jasim, "Exploration of No-Slip and Slip of Unsteady Squeezing Flow Fluid Through a Derivatives Series Algorithm," *Journal of Advanced Research in Fluid Mechanics and Thermal Sciences,* vol. 100, no. 1, pp. 11-29, 2022.

[6] P. Rana, R. Dhanai, and L. Kumar, "Radiative nanofluid flow and heat transfer over a non-linear permeable sheet with slip conditions and variable magnetic field: Dual solutions," *Ain Shams Engineering Journal,* vol. 8, no. 3, pp. 341-352, 2017.

[7] Z. Ullah, and G. Zaman, "Lie group analysis of magnetohydrodynamic tangent hyperbolic fluid flow towards a stretching sheet with slip conditions," *Heliyon,* vol. 3, no. 11, pp. p. e00443,, 2017.

[8] M. Qayyum, H. Khan, and O. Khan, "Slip analysis at fluid solid interface in MHD squeezing flow of Casson fluid through porous medium," *Results in Physics,* vol. 7, p. 732–750, 2017.

[9] A. M. Jasim, "Study effect of MHD on squeezing flow of water-based Casson nanofluid in porous medium between parallel plates," *APL Machine Learning,* vol. 2457, p. 020014, 2023.

[10] R.N. Moghaddam, and M. Jamiolahmady, "Slip flow in porous media," *Fuel ,* vol. 173, pp. 298-310, 2016.

[11] A. M. Jasim, "Study of the impact of unsteady squeezing magnetohydrodynamic copper-water with injection- suction on nanofluid flow between two parallel plates in porous medium," *Iraq Journal of science ,* vol. 36, no. 9, pp. 3909-3924, 2022.

[12] M.J. Babu, and N. Sandeep, "UCM flow across a melting surface in the presence of double stratification and cross-diffusion effects," *Journal of Molecular Liquids,* vol. 232, pp. 27-35, 2017.

[13] D. Srinivasacharya, and O. Surender, "Double Stratification Effects on Mixed Convection along a Vertical Plate in a Non-darcy Porous Medium," *Procedia Engineering ,* vol. 127, pp. 986-993, 2015.

[14] S. Ahmad, M. Farooq, M. Javed, and Aisha Anjum, "Slip analysis of squeezing flow using doubly stratified fluid," *Results in Physics,* vol. 9, pp. 527-533, 2018.

[15] D. G. Al-Khafajy and W. N. Al-Delfi, "The peristaltic flow of williamson fluid through a flexible channel," *Iraqi Journal of Science ,* vol. 64, no. 2, pp. 865-877, 2023.

[16] M. Mustafa, T. Hayat, and S. Obaidat, "On heat and mass transfer in the unsteady squeezing flow between parallel plates," *Meccanica ,* vol. 47, pp. 1581-1589, 2012.

[17] Q. Zhao, H. Xu, and L. Tao,, "Unsteady bioconvection squeezing flow in a horizontal channel with chemical reaction and magnetic field effects," *Mathematical Problems in Engineering,* p. e2541413 , 2017.

[18] J. Al-Saif1, and J. Harfash, "Perturbation-Iteration Algorithm for Solving Heat and Mass Transfer in the Unsteady Squeezing Flow between Parallel Plates," *Journal of Applied and Computational Mechanics ,* vol. 5, no. 4, pp. 804-815 , 2019.

[19] N. Bildik, "General Convergence Analysis for the Perturbation-Iteration Technique," *Turkish Journal of Mathematics and Computer Science,* vol. 6, pp. 1-9, 2017.